
Attitude Determination and Control System for AAUSAT



Project Report

Group 625

Alexander L. Skiadas, Malthe Bilgram & Nikolaj H. Sørensen

Aalborg University
Department of Electronic Systems
Fredrik Bajers Vej 7B
DK-9220 Aalborg



AALBORG UNIVERSITY

STUDENT REPORT

Department of Electronic Systems

Fredrik Bajers Vej 7
DK-9220 Aalborg Ø
<http://es.aau.dk>

Title:

Attitude Determination and Control System for AAUSAT

Theme:

Bsc. Control Engineering

Project Period:

Spring Semester 2014

Project Group:

Group 625

Participant(s):

Alexander L. Skiadas
Malthe Bilgram
Nikolaj H. Sørensen

Supervisor(s):

Kirsten M. Nielsen
Jesper A. Larsen

Copies: 5**Page Numbers:** 115**Date of Completion:**

May 28, 2014

Abstract:

Aalborg University has for many years produced student satellites with great success. These satellites (AAUSATs) consist of various modules, each playing a crucial role for the functionality of the satellite. One of these many subsystems is the Attitude Determination and Control System (ADCS).

The goal of the project is to examine whether an ADCS, based on a *classic* control design and the current hardware setup of the AAUSATs, can be applied for use in space. To investigate whether this is possible, various mathematical models and examinations of the satellite and the space environment, have been made, and documented in this report. It became clear quite quickly, that applying classic control theory, to these models, would be something of a challenge. Therefore, a number of assumptions and simplifications have been made in order to design a classical controller. Following this analysis the controller have been designed and developed.

Based on thorough testing, this paper concludes that the developed controller works as designed and intended, but an actual application in space will cause inaccurate behaviour of the satellite due to the assumptions and simplifications made in the design process.

The content of this report is freely available, but publication (with reference) may only be pursued due to agreement with the author.

Preface

This paper is the bachelor project of a group of Electronics and IT students at the 6th semester at Aalborg University. The report describes the analysis, development and construction of a controller for attitude control on a satellite.

In order to read and understand the report, basic knowledge of linear algebra, classical physics and classical controller design.

References appearing in the report are collected in a source list at the end of the report beginning at page *XXXX*. The references are organised using the Harvard method, so a reference in the text is made by a [author, year], which is further explained in the source list where books and articles are listed by author, title, year of publication and page number. Internet sites are indicated by author, date, URL. When sources are placed directly under the headline of a section it means that the source(s) have been used extensively throughout the chapter.

Figures and tables are numbered according to the chapter, for example the first figure in Chapter 7 has the number 7.1, etc. Explanatory text for figures and tables can be found under the given figures and tables.

The paper comes with an attached CD containing data sheets and source code used in the project.

Aalborg University, May 27, 2014

Alexander L. Skiadads Malthe Bilgram Nikolaj H. Sørensen
<askiad11@student.aau.dk> <maljen11@student.aau.dk> <nhsa11@student.aau.dk>

Notation used in the Report

This chapter explains the different mathematical notation used in this paper. Furthermore, it contains an overview of the different symbols and abbreviations used in the report.

0.1 Vectors

The notation used for a vector is a lower case letter written in bold as shown in equation 1.

$$\mathbf{a} = \begin{bmatrix} a_1 \\ a_2 \\ a_3 \end{bmatrix} = \begin{bmatrix} a_x \\ a_y \\ a_z \end{bmatrix} \quad (1)$$

In case the vector is specified with a subscript the notations is as stated in equation 2.

$$\mathbf{a}_b = \begin{bmatrix} a_{b,1} \\ a_{b,2} \\ a_{b,3} \end{bmatrix} \quad (2)$$

Important Vector Relations

The *inner product* or *scalar product* of two vectors is given by equation 3.

$$\mathbf{a} \bullet \mathbf{b} = [a_1, a_2, a_n] \bullet [b_1, b_2, b_n] = \sum_{i=1}^n a_i \cdot b_i = a_1 \cdot b_1 + a_2 \cdot b_2 + \dots + a_n \cdot b_n \quad (3)$$

The *outer product* or *cross product* of two vectors is given by equation 4.

$$\mathbf{a} \times \mathbf{b} = \begin{vmatrix} a_2 & a_3 \\ b_2 & b_3 \end{vmatrix} \cdot \mathbf{u_x} - \begin{vmatrix} a_1 & a_3 \\ b_1 & b_3 \end{vmatrix} \cdot \mathbf{u_y} + \begin{vmatrix} a_1 & a_2 \\ b_1 & b_2 \end{vmatrix} \cdot \mathbf{u_z} \quad (4)$$

Other valuable vector relations that could be important to remember are listed below:

$$\begin{aligned}\mathbf{a} \bullet \mathbf{b} &= \|\mathbf{a}\| \cdot \|\mathbf{b}\| \cdot \cos(\theta) \\ \mathbf{a} \times \mathbf{b} &= \|\mathbf{a}\| \cdot \|\mathbf{b}\| \cdot \sin(\theta)\end{aligned}$$

Important Vectors in the Report

- \mathbf{r} ; The vector pointing from the center of the Earth to the center of a celestial object.
- \mathbf{v} ; The velocity vector of the satellite, in orbit around the Earth.
- $\hat{\mathbf{e}}_{\mathbf{e}}$; Euler's principal axis.

0.2 Matrices

The notation used for a matrix is a upper case letter written in bold as shown in equation 5.

$$\mathbf{A} = \begin{bmatrix} A_{11} & A_{12} & A_{13} \\ A_{21} & A_{22} & A_{23} \\ A_{31} & A_{32} & A_{33} \end{bmatrix} = \begin{bmatrix} A_{xx} & A_{xy} & A_{xz} \\ A_{yx} & A_{yy} & A_{yz} \\ A_{zx} & A_{zy} & A_{zz} \end{bmatrix} \quad (5)$$

In case the matrix is specified with a subscript the notations is as stated in equation 6.

$$\mathbf{A}_b = \begin{bmatrix} A_{b,11} & A_{b,12} & A_{b,13} \\ A_{b,21} & A_{b,22} & A_{b,23} \\ A_{b,31} & A_{b,32} & A_{b,33} \end{bmatrix} \quad (6)$$

The notation for the *transpose* of a matrix is as followed: \mathbf{A}^T .

The notation for the *complex conjugate* of a matrix is as followed: \mathbf{A}^* .

The notation for the *transpose complex conjugate* of a matrix is as followed: \mathbf{A}^{T*} .

The notation for the *inverse* of a matrix is as followed: \mathbf{A}^{-1} .

Important Matrices in the Report

R; The notation used for all rotation matrices. Each rotation matrix will be specified with a subscript indicating the rotation.

C; The notation for a general direction cosine matrix. Used only in a theoretical contexts. The description of these can be seen in A.

0.3 Rotations and Reference Frames

This report makes use of six different coordinate systems or reference frames in which calculations are done in relation to. The six frames are abbreviated as followed:

- ECIRF or ECI Reference Frame; Earth Centered Inertial Reference Frame. Vectors and matrices in this frame are denoted as ${}^I\mathbf{v}$ and ${}^I\mathbf{M}$.
- ECEFRRF or ECEF Reference Frame; Earth Centered Earth Fixed Reference Frame. Vectors and matrices in this frame are denoted as ${}^E\mathbf{v}$ and ${}^E\mathbf{M}$.
- ORF; Orbit Reference Frame. Vectors and matrices in this frame are denoted as ${}^O\mathbf{v}$ and ${}^O\mathbf{M}$.
- SBRF; Satellite Body Reference Frame. Vectors and matrices in this frame are denoted as ${}^S\mathbf{v}$ and ${}^S\mathbf{M}$.
- CRF; Control Reference Frame. Vectors and matrices in this frame are denoted as ${}^C\mathbf{v}$ and ${}^C\mathbf{M}$.
- TRF; Target Reference Frame. Vectors and matrices in this frame are denoted as ${}^T\mathbf{v}$ and ${}^T\mathbf{M}$.

In order to rotate a vector or matrix from one reference frame into another; rotation matrices and quaternions are used. The notation for a rotation is shown in equation 7 for both matrices and quaternions.

$$\begin{array}{lll} \text{from } \mathbf{R} & \text{e.i.} & {}^S\mathbf{R} \\ \text{to } \mathbf{q} & \text{e.i.} & {}^I\mathbf{q} \end{array} \quad (7)$$

0.4 Explanation of symbols

Here follows a listing of important symbols, with following definitions, as they are used in the paper.

A; Area of a surface. Each area is specified by subscript

a; Acceleration (scalar or size). The acceleration of a certain object will be specified with a subscript.

C; Reflection coefficients. Each coefficient is specified with a subscript.

c; The speed of light.

F; Force. Each force will be specified with a subscript.

I; Current. The current through some object will be specified with a subscript.

J; Moment of Inertia. Each moment of Inertia will be specified with a subscript.

L; Angular momentum.

l; The length of an object or surface.

M; Mass. Each mass will be specified with a subscript.

P; Momentum Flux.

v; Velocity (scalar or size). The velocity of a certain object will be specified with a subscript.

θ ; A regular θ indicates the angle of a rotation.

$\theta +$ subscript; A θ with a subscript indicates a specific angle in some case figure/model etc.

ρ ; Atmospheric density.

τ ; Torque. Each Torque will be specified with a subscript.

ω ; Angular velocity. Each velocity will be specified with a subscript.

Contents

Preface	vii
0.1 Vectors	ix
0.2 Matrices	x
0.3 Rotations and Reference Frames	xi
0.4 Explanation of symbols	xii
1 Introduction	1
2 Preliminary Analysis	5
2.1 ADCS Hardware analysis	6
2.2 Actuators	9
2.3 Orbital Mechanics	12
2.4 The Magnetic field of the Earth	20
2.5 Solar Radiation Pressure and Winds	24
2.6 Aerodynamic Torque	27
2.7 Summary	29
3 Specification Requirements	31
3.1 Mission Analysis	31
3.2 Test specification	33
3.3 Summary	34
4 System Design	35
4.1 The Attitude Determination System, A_D	36
4.2 Model of the Satellite, $G(s)$	43
4.3 Summary	49
5 Design of the ACS Controller, $A_C(s)$	51
5.1 Requirements	52
5.2 System Analysis	53
5.3 Design of the Controller in the Laplace Domain	57
5.4 Verification of the Controller	60
5.5 Design- and Controller Corrections (Feed-Forward)	60
5.6 Design of the Controller in Z-Domain	62

5.7	Summary	62
6	Integration and Accept test	63
6.1	Accept Test	63
6.2	Matlab Simulation	65
7	Closure	73
7.1	Conclusion	73
7.2	Further Development	74
	Bibliography	77
A	Matrix Rotation Theory	79
A.1	Direction Cosine Matrix	79
A.2	Euler Angles	80
A.3	Quaternion	82
A.4	Comparison and Conclusion of the Methods	84
B	Journal for measurement of magnetorquers	87
B.1	Purpos	87
B.2	Used equipment	87
B.3	Measurement arrangement	87
B.4	Measurement procedure	88
B.5	Data processing	88
B.6	Results	89
B.7	Error sources	89
B.8	Conclusion	90
C	Jounal of measurement for the inertia matrix	91
C.1	Purpose	91
C.2	Used equipment	91
C.3	Measurement arrangement	91
C.4	Measurement procedure	92
C.5	Results	92
C.6	Error sources	93
C.7	Conclusion	94
D	Controller Results and Simulations	95

Chapter 1

Introduction

On the 4th of October 1957 the satellite known as Sputnik 1 was sent in orbit around the Earth[Wikipedia, 2013]. This historic event opened a whole new world beyond our own planet. In the following decades mankind continued its research within space technology and expansion into space. The result of this has revolutionized our communication methods on earth, given us huge amount of knowledge about stars, Earth itself, other planets and more. Today, this expansion and desire to evolve our space technology is still a highly regarded topic amongst engineers and scientists.

In the last few years, since 2003, the emergence of CUBE satellites have enabled small independently build satellites to get into space. This has given the opportunity for a much wider range of people and organizations to get access to space. These satellites are often also build by off the shelf components, which further enables projects with high amounts of student involvement, as the cost of a satellite is decreased considerably. Further more, this explosion of student satellites have been noticed by ESA (European space association), which have started a program called "*Fly your satellite*" where, if a satellite is successful in completing, will get a paid launch from ESA. The program lets the development go through the same phases as a commercial satellite, with set deadlines and required documentation and testing by ESA. Currently AAU is, due to special events, participating in this program with two satellites.

The AAU satellites consist of a number of different modules which are designed to work *independently* of each other, thereby making the satellite more flexible towards optimization and changes, as long as each module lives up to the mutual interface structure between the modules. Each module contains a subsystem with a specific task, i.e. power management, ADCS (*Attitude Determination and Control System*), payload and so on.

This paper focuses on the design and development of one of the critical subsystems,

within the satellite, namely the ADCS. This system is used to control the satellites orientation, known as attitude, in order to make it point a specific side towards Earth or another any other direction. This feature is very crucial to the functionality of the satellite, whether it is pointing an antenna to a specific point on earth, or pointing a payload towards a specific point.

As this paper is being written the construction of AAUSAT5 has been initiated. It has been decided by the administration of the AAU space program that AAUSAT5 will be made into a copy of AAUSAT3/4. This decision results in two opportunities for the ADCS designed in this project, as follows:

- Examine whether an implementation of a system, e.i. a camera, which functionality is very dependant of the ADCS, can be implemented with the current hardware setup found on AAUSAT3/4/5. This option offers the opportunity to build and actually test the ADCS in a lab or even in space on AAUSAT3, but it does not give the option of choosing new sensors and designing new hardware for the ADCS.
- Build the whole system from the beginning. This solution makes the project very large and widespread, but offers the opportunity of designing a whole new setup with sensors and hardware, which could be implemented on the next AAUSAT. On the downside it does not offer any real testing of the final system, thereby making the project more theoretical. Limited tests can be performed on Earth with the equipment accessible at the university.

It has been chosen by the project group that the option of testing the ADCS, in hopefully a real environment, weights more than the opportunity of designing both a control system and the hardware around. This decision is also made due to the limited time available for the project and the relative group size compared to others that have undertaken this task. To summarize; **it has been decided to re-use the current setup of AAUSAT3/4/5 and focus on the control system, the ADCS, in order to examine if the existing hardware is substantial for implementing a camera. This means that the attitude control part of the ADCS system, is the only part that will be designed and tested, the rest will stay on a theoretical level.**

It has been chosen to design the attitude control using classical control theory as it has been taught. This means that a controller will be designed to control each individual axis of the satellite. To achieve this, it is necessary first to know the system that is to be controlled. This leads to the investigation of the subjects listed below. These will be investigated in the next chapter:

- What hardware systems are implemented on AAUSAT3/4/5?

- How does a satellite move in space? - and how can its orientation, velocity and position, be described?
- What influence does the magnetic field of the Earth have on the satellites behaviour?
- What influence does solar winds and radiation have on the satellites behaviour?
- What influence does air resistance have on the satellites in LEO (low Earth orbit)?

Chapter 2

Preliminary Analysis

This chapter focuses on explaining the environment the satellite will be operating in. To make the ADCS, and control the rotation of the satellite, it is necessary to know which elements within the environment affects the satellite and how they do so. This chapter contains mathematical models and descriptions of the magnetic field of the Earth, the orbital movement of the satellite, the satellites actuator and the main disturbances that affect an object in outer space.

The model of the Earth's magnetic field can be used along with an orbital description in order to predict how the magnetic field is oriented at a given time, by giving the direction and magnitude of the field. This information is vital for knowing how much current the satellites actuators need to generate the needed control torque to align the satellite. The influence of the disturbances provide useful data on how much control torque is needed, from the actuators, in order to hold the satellite still and the excess torque that can be used to turn it. This is also information useful in creating realistic requirements for the satellites performance. The orbital description is needed to clarify the different elements compared to each other and also to help calculate the location of the satellite and with the magnetic model find the orientation of the satellite. The following elements will be examined in the given order:

- The Hardware of AAUSAT 4.
- Orbital mechanics.
- The magnetic field of the Earth.
- Solar radiation.
- Aerodynamic torque.
- Actuator.

2.1 ADCS Hardware analysis

[group 13gr632, 2013]

In this section the current hardware design of the AAUSAT 4 will be described. As mentioned, there will not be designed any new hardware in this project, but an analysis of the current hardware will be made. The current hardware is described to give an overview of what sensors and actuators, are available to be used in the later control algorithms.

The complete design of the current ADCS can be seen on figure 2.1. There are currently two individual ADCS systems, ADCS1 and ADCS2. ADCS1 is a simple ADCS with limited sensors and the control algorithm is run on an AVR 8-bit MCU. This system has no pointing capabilities, only the ability to detumble the satellite (slow down the spin around its own axis). The ADCS2 has more advanced sensors and an ARM7 32-bit MCU, which has much greater computational power than the ADCS1. This is the part of the satellite where the system designed in this project could be implemented. The ADCS2 sensors consist of six sunsensors, two gyroscopes and two magnetometers. The actuators used to point the satellites are 6 wound coils placed on the sides of the satellite. These are used in conjunction with the earth's magnetic field to generate a control torque and will be described in more detail later.

Sun sensors

To determine the orientation of the satellite the sun can be used, as it has a constant placement compared to the earth and the satellites orbit. This is done by sun sensors, measuring the position of the sun in some manner. On AAUSAT4 the sun sensors are made from photo diodes. These measure the angle with which the incident sun rays hit the diode. Each sensor consists of two photo diodes measuring the angle of the sun. This is done by having a hole over the diodes, such that the sun will shine equally on the two diodes if the sun is right above the hole (the sunvector is perpendicular to the side.) When the sun vector is tilted away one diode will receive more light than the other and this can in turn be used to calculate the angle. A sun sensor is placed on each side of the satellite and via these it is possible to determine the sun vector (a vector going from the satellites center of mass to the sun). The photo diodes that are used on the AAUSAT4 are SLCD-61N8. These are analogue diodes so there are also included an ADC in the sun sensor design. The ADC being used are of the type ADS1148 and this sets a limit on the update time of the sun sensors. The most important specifications are listed in figure 2.2. Because of the sun sensors design being home made the exact accuracy is not known.

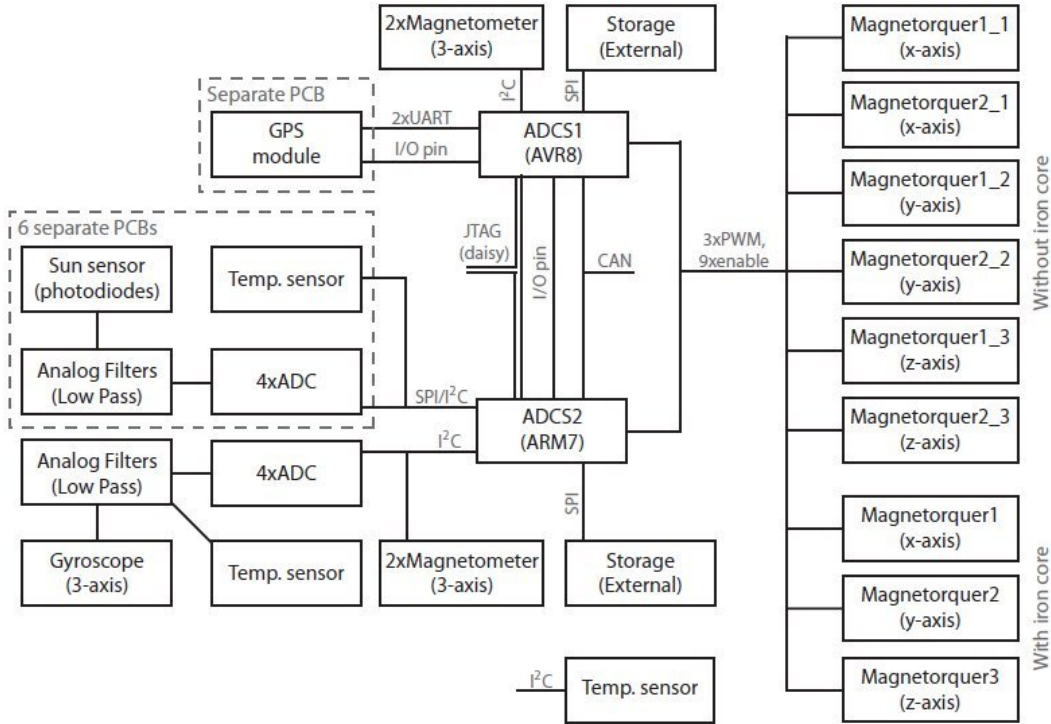


Figure 2.1: Diagram of the entire ADCS showing all hardware components

	SLCD-61N8	ADS1148
Refresh rate	Analogue	2kHz
Acceptance half angle	60°	

Figure 2.2: Specifications for main components used in the sun sensor design.

Gyrosopes

The gyroscopes measure the rotational velocity or rotational orientation on its sensitive axis. These are used to determine the attitude of the satellite during eclipse, when the sun is not visible for orientation. Because the satellite is in LEO it will be behind the Earth some time of its orbit and the sun will not be visible for orientation. The angular velocity of the satellite can then be used to estimate the orientation of the satellite when used in conjunction with the kinematic description of the satellite as seen in chapter 4.2.

The reason why the gyroscopes are not used alone to determine the attitude is due to the initial error, and a build up in error over time if the attitude is determined using only internal sensors. Therefore the gyroscopes and the sun sensors are used in conjunction.

	IDG-1215	ISZ-1215	ADS1115
Refresh rate	Analogue	Analogue	8 – 860Hz
Axis of measurement	x and y 6 z		
Range	$\pm 67^\circ/\text{s}$	$\pm 67^\circ/\text{s}$	
Sensitivity	15mV/ $^\circ/\text{S}$	15mV/ $^\circ/\text{S}$	

Figure 2.3: Specifications for the analogue gyroscopes and the ADC they are attached by.

HMC364	
Refresh rate	5 Hz
Field Range	$\pm 2\text{G}$

Figure 2.4: Specifications for the magnetometer on-board the AAUSAT 3/4/5

To get the whole 3-axis rotation of the satellite a two-axis and a one axis gyroscope is used, the IDG-1215 two-axis gyroscope and the ISZ-1215 single-axis gyroscope. These are both analogue gyroscopes so they are connected to the MCU through a ADC of the type ADS1115. The important data for the gyroscopes are listed in figure 2.3 with the update frequency of the ADC.

Magnetometer

A magnetometer measures the magnetic field it is exposed to, relative to its sensitive axis. On the AAUSAT4, 3-axis magnetometers are used and these give a magnetic field vector.

The magnetometers used on AAUSAT4 are 3-axis magnetometers of the type Honeywell HMC634. These are tilt compensated electronics compasses. It has two different output modes, one where it outputs a compass direction (angle) and a tilt angle and another where it gives a three dimensional vector in the direction of the magnetic field. A extract from the data sheet can be seen in table 2.4. The magnetometer is used to give an accurate measurement of the magnetic field available to create the control torque to align the satellite. The magnetic field vector can also be used inversely with the Earth's magnetic field model and help give a better determination of the attitude. This method of orientation is very advantageous because it also works during eclipse; the time the satellite is in darkness from the sun, behind the Earth.

Magnetorquers

The only actuators on AAUSAT 4 are the three sets of magnetorquers. Each magnetorquer consist of two coils, which makes one coil located on each side of the satellite. The placement on the sides makes the three magnetorquers perpendicular to each

Coils	
Windings	250
Wire thickness	0.1 mm
Dimensions	7.5 x 7.5 cm
Number of coils	6
Wire material	copper

Figure 2.5: Specification for the coils used in the magnetorquers.

other and therefore able to actuate in all directions. On figure 2.7 the configuration of the magnetorquers can be seen.

To create a control torque, current is feed through the coils and this generates a magnetic field. This interacts with the Earth's magnetic field and tries to align according to Laplace law. This is explained further in the next section about the actuators of the satellite. The use of magnetorquers is possible because the satellite is in LEO, where the earth's magnetic field is strong enough to be used to create a considerable torque on the satellite. The coils used on the AAUSAT4 are made specifically for the satellite and have the specifications listed in figure 2.5.

2.2 Actuators

As described in 2.1 the only actuators on the satellite are the magnetorquers which are made up of coils. The way a control torque can be created from these coils is described by Laplace's law in 2.1.

$$F = B \cdot I \cdot l \cdot \sin(\theta) \quad (2.1)$$

where:

F is the force generated.

B is the magnetic field strength.

I is the current through the conductor.

l is the lenght of the conductor.

θ is the angle between the conductor and the magnetic field.

The current through the magnetorquers can be control by a PWM signal from the ARM7 MCU and the AVR 8 bit MCU both located on the ADCS print, the connection can be seen on 2.1. There is a limitation to how high the duty cycle can go of the signal, to ensure the disturbance on the magnetometers is minimal. The maximum duty cycle is 88 %.

To compute the control torque another version of Laplace law is used including the cross product of the two magnetic field vectors instead of the angle between them. This gives the force as a vector product of the magnetic field and the current in the wire elements of the coils.

$$\mathbf{F} = \mathbf{B} \times \mathbf{I} \cdot l \quad (2.2)$$

Where:

- B is the earth's magnetic field
- I is the current through the wire
- l is the length of the wire

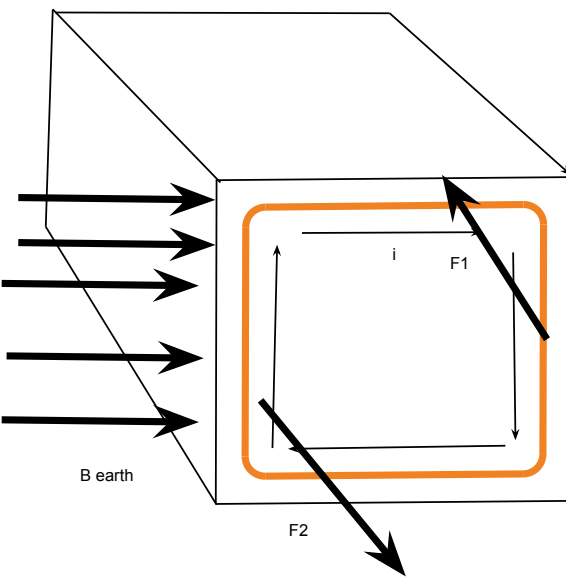


Figure 2.6: Figure the magnetorquers and the forces that act upon it when a magnetic field is present.

In the case where the magnetic field is aligned with the current going through the bottom and top of the coil, the force created through these two wire elements will be zero as it is seen in 2.1 when theta becomes 0 degrees.

This means the only force created is F_1 and F_2 which creates a turning torque on the satellite around the center of the magnetorquer. The forces can be seen on figure 2.6. This means the torque created on the magnetorquer can be described as:

$$\tau = \frac{1}{2} \cdot (F_1 + F_2) \quad (2.3)$$

where:

τ is the torque created

F are the force

l is the length of the sides of the magnetorquer, and the length from the center to the side is half of l .

This equation can be expanded and simplified by inserting 2.2 into 2.3.

$$\tau = \frac{1}{2} \cdot (B \times (I \cdot l) + B \times ((-I) \cdot l)) = A \cdot (B \times I) \quad (2.4)$$

Where: A is the area enclosed by the coils used in the magnetorquer.

This is the way to calculate the torque created by a current running through one wire element of the coil. The magnetorquer can be seen as many wire elements running in parallel and thus to get the full torque that can be created by a magnetorquer the number of windings in the coils can thus be applied to the equation:

$$\tau = A \cdot N \cdot (B \times I) \quad (2.5)$$

To calculate the control torque that can be generated a few other aspects has to be considered. There is a maximum duty cycle on the satellite of 88%. Also for the worst case, where a lot of torque is needed to be applied to align the satellite, is it tumbling in space and it is assumed that the average angle between the Earth's magnetic field and the magnetorquers is $\frac{1}{\sqrt{2}}$, the RMS value. The maximum current that can be feed through the magnetorquer is 20 mA.

This gives a total control torque that can be generated around one axis with one magnetorquer of $2.427 \cdot 10^{-5}$ Nm

This is very close to the aerodynamic torque. Take in mind though, this was under the worst conditions, and when the satellite is not tumbling it might be able to generate a greater torque because the angle between magnetic fields and the satellite will change more slowly.

The way the direction of the control torque is controlled is by passing power through the various magnetorquers. These are defined as M_x , M_y and M_z . Through these run

the current to create the desired control torque, this current is defined as I_x , I_y and I_z . These magnetorquers are named after the axis in the SBRF, see 2.3, that they are perpendicular to. This means that in order to rotate around the x-axis in the SBRF it is necessary to use the y and z magnetorquer, by adjusting the I_y and I_z currents. Because each coil exerts a force in two directions it is expected to get some cross contributions, meaning that one magnetorquer will both align the desired side and distort the other sides at the same time. The placement of the magnetorquers and the way the current runs through them can be seen on figure 2.7.

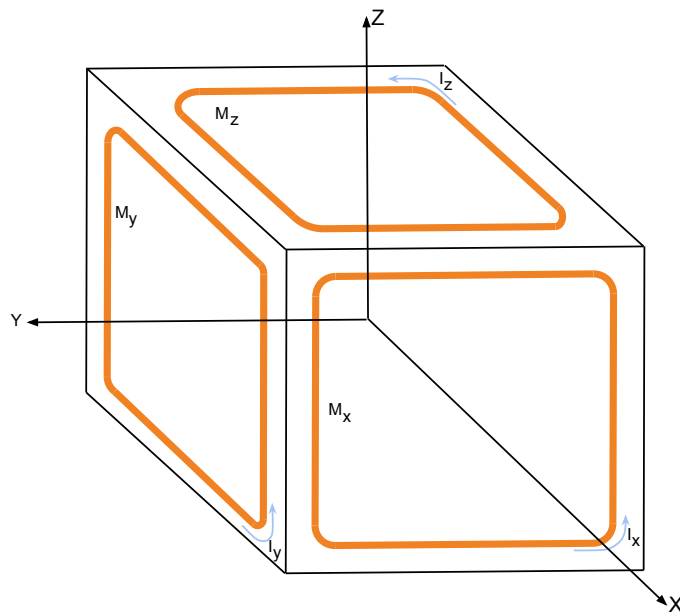


Figure 2.7: Figure the coils of the magnetorquers present on three visible sides of the satellite, the organge is the placement of the coils. The arrows show the way the current runs through the coils. The coordinate system is the SBRF.

This model for the magnetorquers has been verified by test. The test can be found in appendix B, where an experiment was carried out to see if the force created when passing current through a wire in a magnetic field is true. It was found to hold, and thus this is used in the development of the controller.

2.3 Orbital Mechanics

This section examines the mathematics necessary to describe the movement, position and velocity, of objects in space. In order to achieve this two things are required. First each object and region in space must be divided into different coordinate systems or reference frames. This is done in order to describe the different orientation of

different objects relative to one another. All coordinate systems are described by three right-hand unit vectors in the three dimensional space. Secondly, a number of parameters, known as *Keplerian orbit elements*, must be derived to give a mathematical description of the reference frames, in order to examine how they work together. The examination of these problems will be done in the given order;

- Reference Frames - 6 Frames.
- Keplerian Elements.

The subsequent sections are based on the following references and sources [Noton, 1998],[Peter Fortescue & Swinerd, 2003] and [group 13gr632, 2013].

Earth Centered Inertial Reference Frame (ECIRF)

This reference frame has its origin in the center of the Earth. The X-axis goes through the equator and points towards the Sun at the vernal equinox (an astronomic phenomenon where the Sun and the Earth are aligned in a way so a straight line can be drawn from the center of the Sun trough equator to the center of the Earth). The Z-axis of the ECI plane goes through the geographical North- and South pole of the Earth, pointing in the direction of the North pole. The Y-axis is the right hand cross product of the Z- and X-axis. Figure 2.8 shows the graphical explanation of this reference frame.

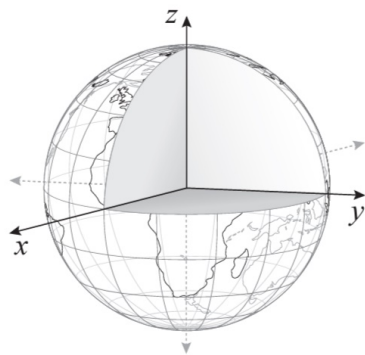


Figure 2.8: The orientation of the three axis in the ECI Reference Frame.

The ECI Reference Frame is used to describe the position and velocity of celestial objects (moons, planets, satellites etc.) in relation to the Earth. Matrices and vectors in this reference frame will be denoted with the following notation $\mathbf{^I M}$ and $\mathbf{^I v}$.

Earth Centered Earth Fixed Reference Frame (ECEFRF)

This reference frame is much similar to the ECIRF. The origin and Z-axis of this plane is the same as in the ECI Reference Frame. This time though, the X-axis goes through the Earth at the point where the Greenwich meridian and equator crosses each other. The Y-axis is once again the right hand cross product of the Z- and X-axis.

The ECEF Reference Frame is used to describe the position of objects with a fixed orientation in relation to the Earth. Objects with a fixed orientation includes mission control centres, antennas and parabolas on Earth and more. Matrices and vectors in this reference frame will be denoted with the following notation $^E\mathbf{M}$ and $^E\mathbf{v}$.

Orbit Reference Frame (ORF)

This reference frame has its origin in the center of mass of the orbiting element, in this case a satellite. The Z-axis points in the direction of the center of mass of the Earth and X-axis is aligned with the velocity vector of the satellite. Once again the Y-axis is the right hand cross product of the Z- and X-axis. Figure 2.9 shows a graphical explanation of the ORF.

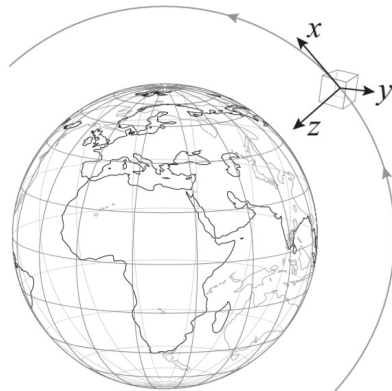


Figure 2.9: The figure shows the orientation of the three axis ORF plane.

As for the ECIRF, the ORF is used to describe the position and velocity of an object in relation to the satellite. Matrices and vectors in this reference frame will be denoted with the following notation $^O\mathbf{M}$ and $^O\mathbf{v}$.

Satellite Body Reference Frame (SBRF)

This reference frame is a bit more complex than the others because it depends on the design of each individual satellite, or object, instead of being more generally specified like the other frames. This frame describes the position of the elements within the satellite, just as the ECEF reference frame describes elements on the Earth. Since most satellites are built differently, their SBRF orientation also varies and therefore a SBRF from one satellite can normally not be used for another.

Because all AAU satellites have the same geometrical construction and primary elements, it is possible to use the same SBRF as of AAUSAT3 and AAUSAT4. Furthermore, since AAUSAT5 is a copy of AAUSAT4 then it is acceptable to use the same SBRF. *The X-axis of the frame is pointing in the direction along the batteries while the Z-axis is pointing orthogonally in the opposite direction in the plane spanned by the antennas, and the Y-axis is the right hand cross product of the Z- and X-axis*[group 13gr632, 2013]. Matrices and vectors in this reference frame will be denoted with the following notation \mathbf{sM} and \mathbf{sv} . The SBRF can be seen on figure 2.10.

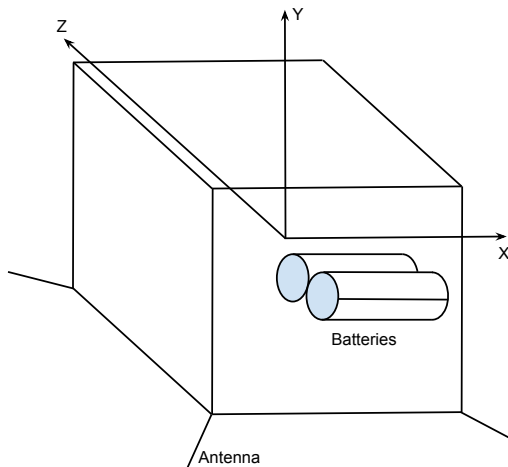


Figure 2.10: This figure shows the SBRF in the satellite with the batteries and antennas.

Control Reference Frame (CRF)

The CRF is the reference frame where the controller works. All regulation will be done in this reference frame and then transferred to the SBRF. This reference frame is dependant on the moment of inertia for the satellite and will be derived in chapter 4.2.

Target Reference Frame (TRF)

This reference frame has its origin in the center of mass just as the ORF and SBRF. The Z-axis is a line which goes through the mission control center (AAU) and the center of mass of the satellite always pointing away from the mission control center. The X-axis is orthogonal to the Z-axis pointing in the direction in which the satellite travels. Once again the Y-axis is the right hand cross product of the Z- and X-axis.

This reference frame is used to *define* a target for the satellite. In other words, it tell us in which direction we want to point. So when moving the satellite, the goal is to align the SBRF and the TRF planes. Matrices and vectors in this reference frame will be denoted with the following notation ${}^T\mathbf{M}$ and ${}^T\mathbf{v}$.

The Keplerian Elements

In order to combine the above mentioned reference frames, mathematical parameters are necessary to express the position and velocity of the satellite, and hence place the SBRF within the ECIRF. These different parameters are known as *Keplerian Elements*. The Keplerian elements can be derived by the 3 laws of Kepler describing planetary movement or mathematically by Newtons laws of motion and his law of gravitation. This derivation is also referred to as *The Two-Body Problem*.

Consider two object in an inertial reference frame as figure 2.11 shows. According to the law of gravitation made by Newton, the forces affecting the masses can be expressed by equation 2.7.

$$\mathbf{F}_1 = \frac{G \cdot M_1 \cdot M_2}{r^2} \cdot \frac{\mathbf{r}}{r} \quad (2.6)$$

$$\mathbf{F}_2 = \frac{G \cdot M_1 \cdot M_2}{r^2} \cdot \frac{-\mathbf{r}}{r} \quad (2.7)$$

Where G is the gravitation constant, M_1 and M_2 is the mass of the two objects, \mathbf{r} is the vector between the two masses and thereby describing both distance and direction, where r simply is the numerical value of \mathbf{r} and thereby only describing the

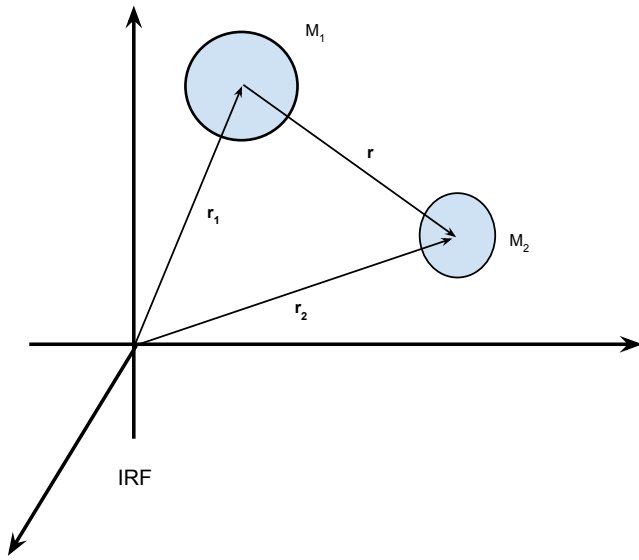


Figure 2.11: An illustration of the two-body problem within an Inertial Reference Frame

distance between the masses. Furthermore, if using the second law of Newton, the forces F_1 and F_2 can also be expressed by equation 2.9

$$\mathbf{F}_1 = M_1 \cdot \ddot{\mathbf{r}}_1 \quad (2.8)$$

$$\mathbf{F}_2 = M_2 \cdot \ddot{\mathbf{r}}_2 \quad (2.9)$$

By noting on figure 2.11 that $\mathbf{r} = \mathbf{r}_2 - \mathbf{r}_1$, equation 2.7 and 2.9 can be combined into equation 2.10

$$\ddot{\mathbf{r}} + \frac{G \cdot (M_1 + M_2)}{r^2} \cdot \frac{\mathbf{r}}{r} = 0 \quad (2.10)$$

If we now assume that the mass of one of the bodies are much bigger then the other, $M_1 \gg M_2$, consider the case where a satellite is in orbit of the Earth as an example, then equation 2.10 can be simplified into equation 2.11:

$$\ddot{\mathbf{r}} = -\frac{G \cdot M_1}{r^2} \cdot \frac{\mathbf{r}}{r} \quad \rightarrow \quad -\frac{\mu \cdot \mathbf{r}}{r^3} \quad (2.11)$$

Where $\mu = G \cdot M_1$. Now consider the vector \mathbf{h} which describes the angular momentum pr. unit mass. The angular momentum is constant due to the fact that only conservative forces affect the masses. \mathbf{h} is defined by equation 2.12, furthermore, one should notice that \mathbf{h} is normal to both \mathbf{r} and $\dot{\mathbf{r}}$ and therefore it is also normal to the plane of motion.

$$\mathbf{h} = \mathbf{r} \times \frac{d\mathbf{r}}{dt} \quad (2.12)$$

Equation 2.13 can be derived by taking the vector product of equation 2.11 and 2.12.

$$\ddot{\mathbf{r}} \times \mathbf{h} = - \left(\frac{\mu}{r^3} \right) \cdot \mathbf{r} \times (\mathbf{r} \times \dot{\mathbf{r}}) = \mu \frac{d}{dt} \left(\frac{\mathbf{r}}{r} \right) \quad (2.13)$$

The vector solution to 2.13 can be found by integration, this solution is also known as *The Vector-Equation of Orbit*. Because \mathbf{h} is constant the equation can be integrated directly, which gives equation 2.14.

$$\dot{\mathbf{r}} \times \mathbf{h} = \mu \cdot \frac{(\mathbf{r} + \mathbf{r} \cdot \mathbf{e})}{r} \quad (2.14)$$

Where \mathbf{e} is called the *eccentricity vector*. To get the *Standard-Equation of Orbit*, one simply takes the inner product of equation 2.14 with \mathbf{r} and solves with regard to r , thereby getting equation 2.15.

$$r = \frac{\left(\frac{h^2}{\mu} \right)}{1 + e \cdot \cos(\Theta)} \quad (2.15)$$

Where Θ is the angle between the vectors \mathbf{r} and \mathbf{e} . This equation (2.15) demonstrates or *proves* the first law of Kepler. For the eccentricity constant, $e = 0$, the orbit of the small object around the first object is circular. For $e < 1$ the orbit is elliptical, for $e = 1$ the orbit is a parabola and for $e > 1$ the orbit is a hyperbola as figure 2.12 shows.

Furthermore, figure 2.12 illustrates the first three of the six Keplerian Elements, which are defined as followed:

- a , called *the semi-major axis*, which describes the size of the ellipsis in form of the distance from the centre to the edges.

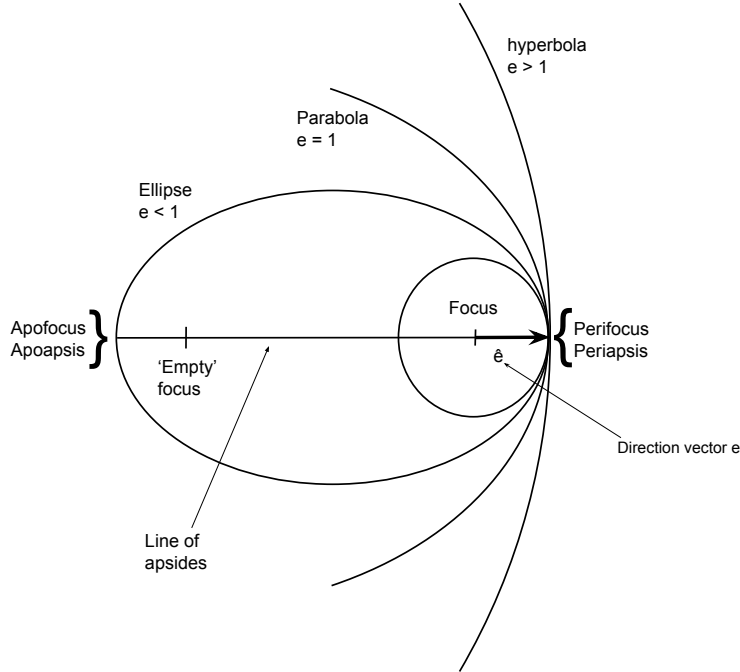


Figure 2.12: The figure shows an illustration of the different types of orbit along with the first 3 Keplerian Elements, e , a and θ .

- e , called the *the eccentricity constant*, which describes the shape of the ellipsis.
- Θ , called *the true anomaly*, which is the angle between the motion vector \mathbf{r} and the eccentricity vector \mathbf{r}_e .

In order to determine the last three Keplerian Elements, it is necessary to take the ECI Reference Frame into account in this model, as figure 2.13 shows. The intersection line between the equatorial plane and the orbit plane, is called the line of nodes, which intersects in two points: *The ascending node*, where the satellite crosses the equatorial plane going from south to north, and *the descending node*, where it crosses the plane going from north to south. The three last elements are given as followed:

- Ω , called *the ascending node angle*, which describes the east-west orientation of the ascending node, which is the angle measured from the equatorial plane, east ward from the ECI x-axis, to the ascending node.

- ω , called *the argument of periapsis*, which describes the rotation of the ellipse within the orbital plane.
- i , called *the angle of inclination*, which describes the angle from the equatorial plane to the orbit plane.

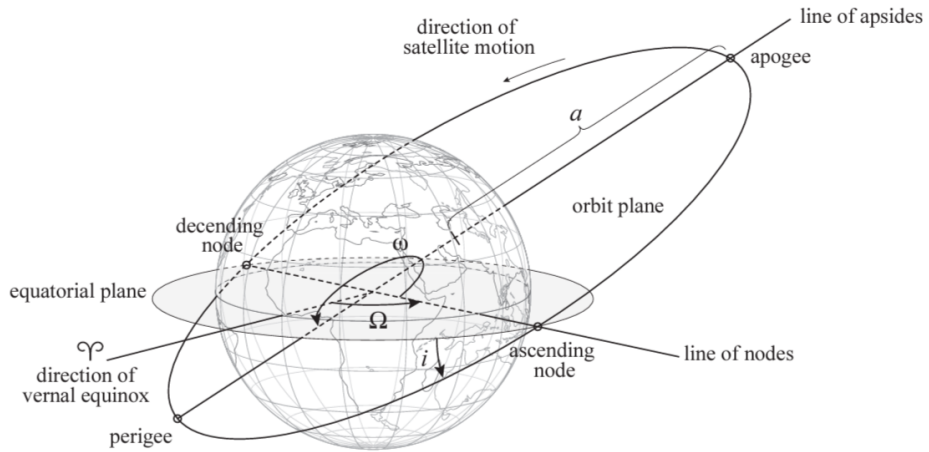


Figure 2.13: The figure shows the orbital movement of a satellite within the ECI Reference Frame.

2.4 The Magnetic field of the Earth

The magnetic field of the Earth has been a mystery to scientist for decades it and still is. Though scientist do agree that the magnetic field resembles that of a bar magnet, tilted 11 degrees from the spin axis as figure 2.14 shows. There is just one problem with this picture; The Curie temperature of iron is about 770 degrees Celcius, and the core of the Earth is hotter than that, which makes it non-magnetic[Hyperphysics, 2014]. This problem will be explained later in the section.

Magnetic fields decay over time and it can be shown that the magnetic field of the Earth would disappear in about 15000 years, if mechanism to regenerate it[Geomag, 2013] did not exist. Throughout the years, many theories have been postulated for what could be generating the magnetic field that surrounds the Earth, but as of now there is only one that is considered plausible. This theory can be compared to mechanism of a dynamo - a mechanism for converting mechanical energy to electric energy[Geomag, 2013].

To get a better understanding about how the dynamo effect would work within the Earth, it is necessary to look at the different layers of the Earth as figure 2.15 shows. The interesting layers in this context is the outer core and the inner core. The

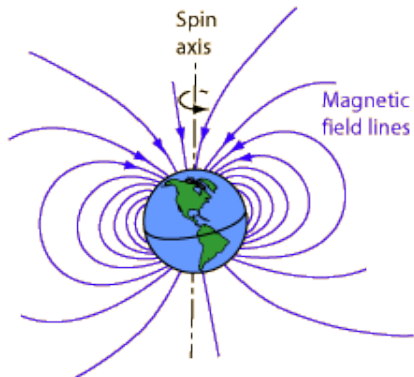


Figure 2.14: The figure shows the magnetic field of the Earth[Hyperphysics, 2014].

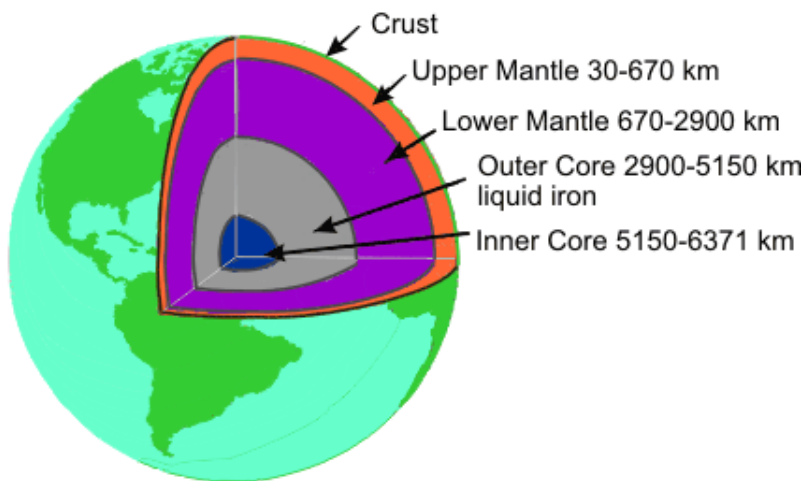


Figure 2.15: The figure shows the different layers that the Earth consist of[Geomag, 2013].

temperature of the inner core is approximately 5430 degrees celcius, but due to the high pressure it is solid and is primarily composed of iron. The outer core though, is liquid, due to lower pressure and temperature. Furthermore, it is in constant motion due to both the rotation of the Earth and of convection. This convection is driven by an upward motion of the light elements contained in the outer core, as the heavier elements freeze onto the inner core[Geomag, 2013]. The actual process that explains how the magnetic field is produced in an environment such as the Earth is highly complex. However, the basic concepts are fairly easy to comprehend. There are some conditions that must be met in order for the possibility of a magnetic field being generated under such circumstances:

- There must be a conducting fluid
- There must be enough energy to cause the fluid to move with sufficient speed

and with the appropriate flow pattern

- There must be a "seed" magnetic field

These condition are all met in the outer core of the earth. For the first condition, there is the molten iron, that the outer core consists of, which is a good conductor. The second condition is the convection that was described earlier. The convection motion and the rotation of Earth makes the necessary flow pattern. Then there is only the last condition that has to be met; the *seed* magnetic field. There are other magnetic fields present in our solar system, for instance the field of the sun. This works as the *seed* magnetic field. When the magnetic field of the sun passes through the molten iron in the inner core of the Earth, an electric current is generated by the magnetic induction process. This new electric field will create a magnetic field and given the right relationship between the magnetic field and the fluid flow, this newly generated magnetic field will be able to reinforce the initial field[Geomag, 2013]. This process will keep on going for as long as there is sufficient fluid motion in the outer core. But this is still just considered a plausible explanation to the question about how the magnetic field of the Earth is generated.

For satellite matters, the magnetic field of the Earth is strong enough to measure, but it is not equally strong all over the globe. It is strongest around the magnetic poles where it reaches around $60 \mu\text{T}$, but only about $31 \mu\text{T}$ at the equator [Wisegeek, 2014]. This problem will be looked further into in the following section.

International Geomagnetic Reference Field (IGRF)

As mentioned, when sending a satellite into space, it is necessary that it contains a mechanism to control the satellites orientation towards the Earth. But in order to do so, a model of the magnetic field of the Earth is a necessity, because the magnetic field is not equally strong all over the globe, especially when the goal is to turn the satellite with magnet torques. The satellites ADS (attitude control system) need know magnetic field vector for attitude determinition, so it knows how to adjust, and how it can according to the measured magnetic field strength. A model of the Earth's magnetic field is important for modelling purposes and also for the ADCS to compare the measured magnetic vector to one from the model to determine the attitude. There are several models describing the magnetic field of the Earth in different ways. This paper will only focus on one of these models, the one called *The International Geomagnetic Reference Field* (IGRF).

The IGRF is a model of the magnetic field of the Earth developed by the International Association of Geomagnetism and Aeronomy Working Group V-MOD. The model is developed by various magnetic field modellers from different parts of the world. Because the IGRF is based on a mathematical description, it is not directly

describing the magnetic field generator, therefore it is frequently updated; every fifth year approximately. At this moment it is at its 11th generation, but since the current model only works until 2015, the IAGA Working Group V-MOD have begun preparations for the 12th generation of the IGRF[IUGG, 2000].

This leads to the actual IGRF 11th generation model, which consists of various mathematical models, where each model contains of a set of Gauss coefficients. The current IGRF model can be seen on Equation 2.16.

$$V(r, \theta, \lambda, t) = a \sum_{n=1}^N \left(\frac{a}{r}\right)^{n+1} \sum_{m=0}^n (g_n^m(t)\cos(m\lambda) + h_n^m(t)\sin(m\lambda)) P_n^m(\cos(\theta)) \quad (2.16)$$

Where:

- g_n^m and h_n^m is the numerical Gauss coefficients.
- t is the time.
- r is the radial distance from the centre of the earth in kilometers.
- $a = 6371.2\text{km}$ is the magnetic spherical radius.
- θ is the geocentric co-latitude ($90\text{ deg} - \text{lattitude}$).
- λ is east longitude.
- $P_n^m \cos(\theta)$ is the Schmidt semi- (or quasi-) normalized associated Legendre functions of degree n and order m .

From Equation 2.16 the following derivatives can be obtained:

$$X = \frac{1}{r} \frac{\partial V}{\partial \theta} \quad (2.17)$$

$$Y = -\frac{1}{r \sin(\theta)} \frac{\partial V}{\partial \lambda} \quad (2.18)$$

$$Z = \frac{\partial V}{\partial r} \quad (2.19)$$

The Equations in 2.17, 2.18 and 2.19 are used to calculate the magnetic field components. For better understanding figure 2.16 show the seven elements of the magnetic

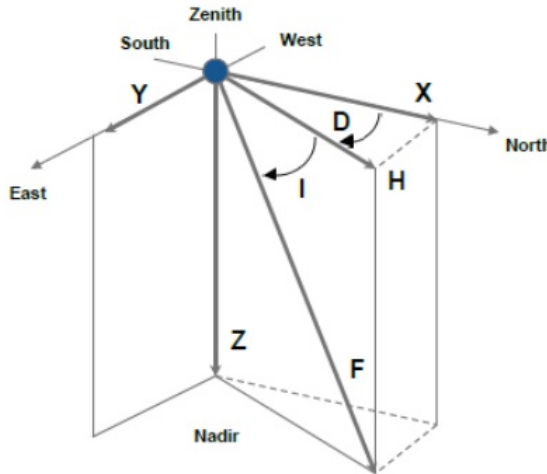


Figure 2.16: The 7 elements of the magnetic field Survey [2009].

field of the Earth, herein X, Y and Z are contained. Where X is the northerly intensity, Y is the easterly intensity and Z is the vertical intensity. Together the three Equations 2.17, 2.18 and 2.19, the magnetic field vector of the Earth. All intensities are measured in nano Tesla. The other elements on Fig 2.16 are:

- H: The horizontal intensity.
- F: The total intensity to a point.
- I: The inclination angle.
- D: The declination angle.

The IGRF gives us the possibilities of calculating the different intensities of the magnetic field of the Earth, compared to our position in space or on Earth. Since these calculations can be very comprehensive, a MATLAB script that calculates the magnetic field vector have been acquired. The script is made by the working group V-mod. The script will be put on a CD, delivered with the report.

2.5 Solar Radiation Pressure and Winds

[Sidi, 1997][Wertz, 1999]

The disturbance of the sun consists of both the solar radiation pressure and solar winds. The solar radiation pressure consists of all the electromagnetic waves emitted by the sun. Solar winds consists of ionized electrons and nuclei emitted from the

Altitude [km]	Solar radiation [W/m ²]	Earth reflectance [W/m ²]	Earth radiation [W/m ²]
500	1358	600	150
1000	1358	500	117
2000	1358	300	89
4000	1358	180	62
8000	1358	75	38
15000	1358	30	14
3000	1358	12	3
60000	1358	7	2

Figure 2.17: Intensity of radiation pressure for different sources.

sun. The main disturbance comes from the solar radiation pressure which is 100 or 1.000 times bigger than the disturbance from solar winds, especially in lower orbits where most of the ionized particles are diverted by the magnetic field of the Earth. The Earth also emits radio waves as well as a reflection from the sun, there is also a reflection of the sun's from the moon, but these are so small compared to the direct solar radiation pressure that they are omitted. The radiation pressure from different bodies can be seen in figure 2.17.

The mean value for the solar energy flux over all wavelengths is proportional to the inverse square of the distance to the sun. This means for a satellite in LEO this value can be considered constant as the distance to the sun does not vary significantly. The mean momentum flux, P, can then be expressed as:

$$P = \frac{F_e}{c} \quad \left[\frac{W}{m^2} \right] \quad (2.20)$$

where:

F_e is the solar constant

c is the speed of light

This is proportional to the force which is acted upon the satellite. The incident solar radiation affecting the satellite does so in three different ways. The radiation is either absorbed, reflected specularly or reflected diffusely, each can be seen on figure 2.18. The differential radiation force of the absorbed incident radiation is given by:

$$dF_{\text{absorbed}} = -P \cdot C_a \cdot \cos(\theta_{\text{sun}}) \cdot \hat{S} \cdot dA \quad (0^\circ < \theta_{\text{sun}} < 90^\circ) \quad (2.21)$$

where:

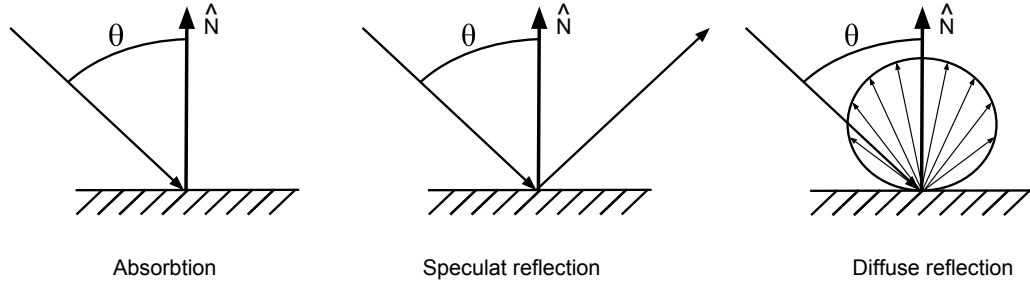


Figure 2.18: Here each of the reflection types are seen: Absorption, specular and diffuse.

P is the momentum flux given in 2.20

C_a is the absorption coefficient

dA is an element area with outward unit normal vector \hat{N}

\hat{S} is the unitvector from the spacecraft CoM (center of mass) to the suns CoM

θ_{sun} is the angle between \hat{S} and \hat{N}

When the angle θ_{sun} becomes negative this means the side of the satellite is turned away from the sun and is therefore not hit by any incident radiation from the sun. Likewise there is a equation for the differential force from the specularly reflected incident radiation given by:

$$dF_{\text{Specular}} = -2P \cdot C_s \cdot \cos^2 \theta_{\text{sun}} \cdot \hat{N} \cdot dA \quad (0^\circ < \theta_{\text{sun}} < 90^\circ) \quad (2.22)$$

where:

C_s is the specular reflection coefficient

With diffusely reflected incident radiation the reflection of the radiation is distributed over all directions. The distribution is proportional to $\cos(\theta_{\text{sun}})$ where θ_{sun} is the angle between the reflected radiation and \hat{N} . The equation given for the differential force from the diffusely reflected incident radiation is given by:

$$dF_{\text{Diffuse}} = PC_d \left(-\frac{3}{2} \cos(\theta_{\text{sun}}) \hat{N} - \cos(\theta_{\text{sun}}) \hat{S} \right) dA \quad (0^\circ < \theta_{\text{sun}} < 90^\circ) \quad (2.23)$$

where:

C_d is the diffuse reflection coefficient

These three equations 2.21 to 2.23 can be combined into one equation for the total radiation force acted upon the satellite by the solar radiation. It is assumed that all solar radiation will interact with the satellite either through absorption, specular or diffuse reflection, therefore it is assumed that $C_a + C_s + C_d = 1$. Now it is possible to determine the total differential force by:

$$dF_{\text{total}} = -P \int dF_{\text{absorbed}} + dF_{\text{Specular}} + dF_{\text{Diffuse}} \quad (2.24)$$

$$= -P \int \left[(1 - C_s - C_d) \hat{S} + 2C_s \cdot \cos(\theta_{\text{sun}}) \cdot \hat{N} + \frac{2}{3} \cdot C_d \cdot \hat{N} + C_d \cdot \hat{S} \right] \cos(\theta_{\text{sun}}) \cdot dA \quad (2.25)$$

$$= -P \int \left[(1 - C_s) \cdot \hat{S} + 2 \cdot \left(C_s \cos(\theta_{\text{sun}}) + \frac{1}{3} \cdot C_d \right) \cdot \hat{N} \right] \cdot \cos(\theta_{\text{sun}}) \cdot dA \quad (2.26)$$

For the satellite the area A is the sides that lie within ($0^\circ < \theta < 90^\circ$) and are affected by the sun. When the force contributed from each side are found and summed up as in 2.26 the solar radiation torque can be found. This is given by:

$$\tau_{\text{solar}} = \int R \times dF_{\text{total}} \quad (2.27)$$

where:

r is the vector from the spacecraft CoM to the incident side

With all of the above equations the torque from the sun's radiation can be calculated. The worst torque experienced on one side will be when all these worst case scenarios are met:

$$P = 4.52 \cdot 10^{-6}$$

$$1 - C_s = 1$$

$$C_s \cos(\theta_{\text{sun}}) = 1$$

$$\frac{1}{3} C_d = \frac{1}{3}$$

$$\cos(\theta_{\text{sun}}) = 1$$

$$A = 113 \cdot 10^{-6}$$

With these numbers inserted into the 2.27 the worst torque can be found. This gives a maximum torque on a side of $2.046 \cdot 10^{-11} \text{ Nm}$.

2.6 Aerodynamic Torque

[Sidi, 1997][Wertz, 1999]

Due to the molecules still present in the upper atmosphere the satellite will periodically collide with these and due to the low friction environment in space these molecules will create a torque on the satellite. The magnitude of the force acted upon the satellite is proportional to the density of the atmosphere. Because the atmosphere is denser closest to Earth, the lower the orbit the bigger is the aerodynamic disturbance. For satellites orbiting earth under approximately 400 km the aerodynamic disturbance will be the main disturbance. With the great speed of the satellite the molecules that interact will only be hitting the *front* of the satellite, therefore it can be seen as a plane flying through space. This plane is the cross area of the satellite perpendicular to the direction it travels. An illustration of this can be seen on figure 2.19

The force of the aerodynamic disturbance is given by:

$$dF_{\text{Aero}} = -\frac{1}{2} \cdot C_D \cdot \rho \cdot v^2 \cdot (\hat{n} \cdot \hat{v}) \cdot \hat{v} \cdot A \quad (2.28)$$

where

C_D is the drag coefficient

ρ is the atmosphere density at the orbit altitude

\hat{V} is the unit vector of the translatory velocity of the satellite

A is the plane of the projected area in the direction of travel with normal vector \hat{n}

The torque that this applies to the satellite around the CoM is given by:

$$\tau_{\text{Aero}} = \int R \times dF_{\text{Aero}} \quad (2.29)$$

where

r is the vector from the satellite CoM to the plane A

An analysis have been made of cubesats in orbit and their drag coefficients and both AAUSAT-1 and AAUSAT-2 are included in it. Because the AAUSAT's are very similar it is expected that they all have close to the same drag coefficient. From the paper it is also seen that most estimates for cubesat drag coefficients lie within 1 - 4. It is seen that for AAUSAT-2 the coefficient are very closely estimated around 2,5 so this is to be the expected average drag coefficient on the satellite [Oltrogge, 2011]. The plots of the satellites from the paper can be seen in figure 2.20

With this the aerodynamic torque can be computed. The torque can be calculated to be between the best and worst case. It is assumed that the worst drag coefficient

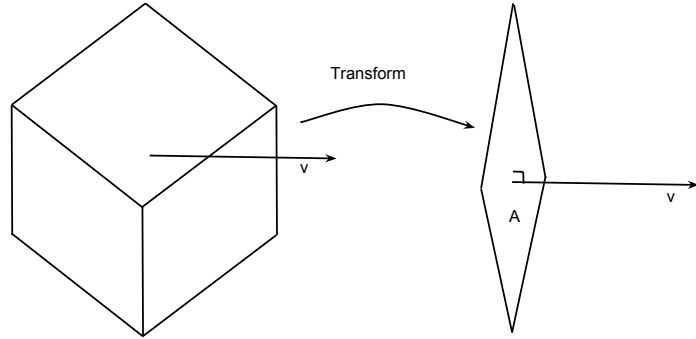


Figure 2.19: Shows how the satellite is transformed to a plane in space. The plane consist of the cross area of the satellite perpendicular to the translatory velocity vector.

is when the satellite faces one side in the direction of motion, and the best drag coefficient when facing a corner in the direction of motion. The best drag coefficient is set to 1,5 and the worst is set to 4. The forces created by the atmospheric drag will be:

$$dF_{\text{Aero}} = -\frac{1}{2} \cdot 4 \cdot 3,8 \cdot 10^{-12} \frac{\text{kg}}{\text{m}^3} \cdot (7670 \frac{\text{m}}{\text{s}})2 \cdot 0.01\text{m}^2 = 4.359 \cdot 10^{-6} \quad (2.30)$$

$$dF_{\text{Aero}} = -\frac{1}{2} \cdot 1.5 \cdot 3,8 \cdot 10^{-12} \frac{\text{kg}}{\text{m}^3} \cdot (7670 \frac{\text{m}}{\text{s}})2 \cdot 0.026\text{m}^2 = 4.471 \cdot 10^{-6} \quad (2.31)$$

When inserted into 2.29 this yields the torque applied by aerodynamics to the satellite. This is approximately $0.134 \cdot 10^{-6}\text{Nm}$.

2.7 Summary

The different reference frames needed to describe all motion of both the satellite and the Earth are now known. This means it is possible to describe the position of everything in order to design and test the controller. The orbit of the satellite is and the placement of objects on Earth can be described in connection to the satellite

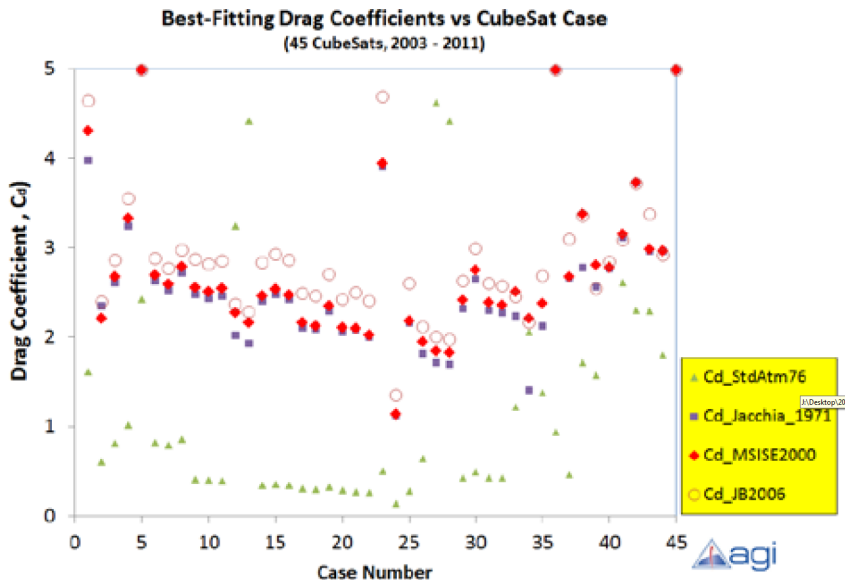


Figure 2.20: From An Evaluation of CubeSat Orbital Decay, aausat 1 is nr. 5 og aausat-2 is nr. 20 on the plot

making it possible for it to point. Furthermore with the main disturbances and their nature described it is possible to find the best way to counter act these. These will furthermore be used as models in the simulation environments that will be used to evaluate the quality of the controller design. As it can be seen the aerodynamic torque is by far the largest and it is therefore the only disturbance that is included in further development. The description of the IGRF will also be used as a model in later simulation environments used to evaluate the controller. Further more it helps to understand how the magnetic field which is used for actuation on the satellite works.

This leads to the next chapter which will describe the requirements for the controller. This chapter will also focus on what tests will be used to evaluate the controller with respect to these requirements.

Chapter 3

Specification Requirements

In this chapter the different specification requirements for the satellite will be set up as a result of an analysis of the mission. Furthermore, the chapter will contain an elaboration of the different test necessary to verify the different demands to the system. The focus of this chapter can be divided in two parts examined in the following order:

- Mission Analysis
- Accept Test Overview

3.1 Mission Analysis

This section will examine what the requirements would be for a fictive mission using the same hardware as is on board the AAUSAT 3/4/5. To find these requirements it is first necessary to have a description of the mission.

It is desired to put a camera on the satellite, similar to that which was on the AAUSAT 2, in order to take pictures of the different cities of Denmark. It is desired to get the whole city in one picture which means that it should be possible for the camera to be still and pointed accurately enough to capture it. It is assumed that an area of 20 km x 20 km can hold most cities.

The camera was of the type MCM20027 from Motorola. This camera has a view angle of 15° which means its total field of view from the satellite is 30°. With the satellite orbit altitude this gives an area that can be seen from the satellite. Which gives the camera at a 400 km altitude the ability to "see" an area 200 km across the Earth's surface. This means that the satellite should point the camera at earth with

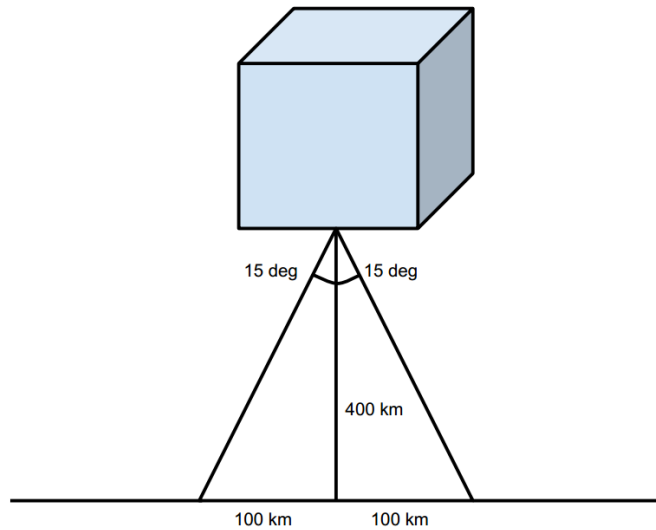


Figure 3.1: This figure illustrates the visible area from the satellite.

a precision of 12 degrees, this is illustrated on figure 3.1. The angles are calculated using basic trigonometry.

To make sure there are several pictures of the spot, pictures will be taken while the satellite is adjusting. To be sure to keep the center of the picture in all pictures, it has been chosen to have an overshoot that will not allow the center of the target point to slip out of the cameras view. In a worst case where a 180 degree turn is needed, 15 degrees corresponds to about 8 %. Therefore this will be the design maximum design target during the design of the controller.

The camera has a frame rate of up to 10 FPS, (frames per second) which means that the camera take a picture very quickly, and thus is it not important for the camera whether the satellite can be still for longer amounts of time as in 6 seconds a satisfactory picture can be taken.

With the fast picture taking time of the satellite should just be able to keep the camera steady for some 6 seconds to take a picture. It is wanted to get the pictures from the satellite taken directly down, and not with too great an angle. An angle of 10 degrees is wanted and this is equal to a time directly over an area of 18 seconds. This is calculated by trigonometry as the satellite is 400 km above Earth and a 10 degree angle. This gives 140 km of travel for the satellite to turn. With a velocity of 7670 km/h this corresponds to 65 seconds. This area is illustrated on figure 3.2.

This means that the satellite should be able to turn completely within 59 seconds, as the worst case scenario is to turn the camera in the opposite direction, a 180 degree turn. This means that the satellite should be able to turn with a speed of 15 degrees

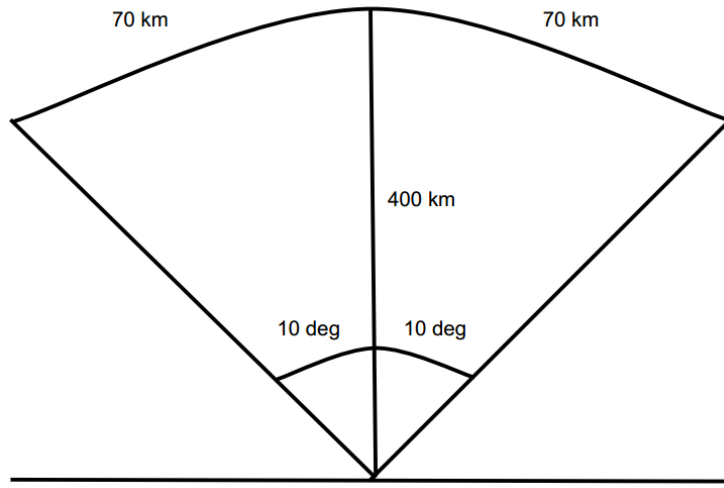


Figure 3.2: This shows the area where the satellite can take an acceptable picture.

/ second.

To sum these requirements up:

- The satellite must be able to point with 2.75 degrees precision.
- Should be able to turn 180 degrees in 59 seconds.
- For a full rotation an average speed of 3 degrees/ second should be obtained.

3.2 Test specification

This section contains a detailed overview and description of the tests necessary to validate the demands that has been setup for the ADCS of the satellite.

The Laboratory Test

The ADCS can be tested in a laboratory by uploading the controller code into a test model of AAUSAT3. The test satellite can then be placed in a magnetic field, generated by a Helmholtz coils, to simulate the environment in which the satellite will be operating in as figure 3.3 shows. It is very important that the satellite *hangs freely* in the field with as little friction as possible. This is done by hanging the satellite model in a connection between two ball magnets.

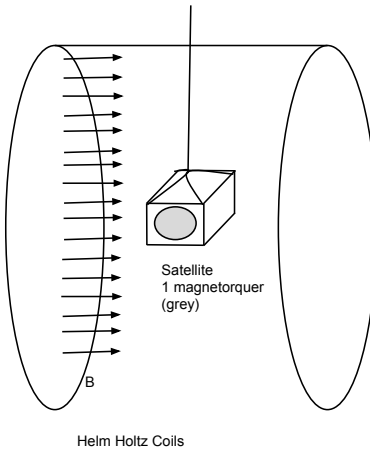


Figure 3.3: The figure shows the setup of the laboratory test using Helmholtz coils and test satellite.

This test may not give the most authentic picture of how well the ADCS works because the environment is far from ideal. However, it can be used to verify the functionality of the controller and how precise the satellite is orientated, because its orientation can be seen and measured in relation to a specific reference point.

The MATLAB Simulation Test

A second test of the system will be done in a MATLAB simulation environment provided by the AAU space team. In this environment the functionality of the ADCS can be evaluated based on a more space like environment which includes all the different disturbances and behaviours of celestial object as described in the previous chapter.

3.3 Summary

In conclusion this chapter has provided an overview of the different operational requirements which will be made into controller specific requirements during controller design. Further more the tests to verify the functionality of the controller are described here. This leads to the final description of the satellite models which are needed to describe the system, such that a controller can be successfully designed.

Chapter 4

System Design

In previous chapters, the disturbances affecting the satellite and how basic orbital movement can be described has been investigated. The main focus of this chapter is to give an overview of the ADCS by explaining the interaction of all the previous examined elements that are found within the ADCS of the satellite. Figure 4.1 gives an overview of the ADCS, where:

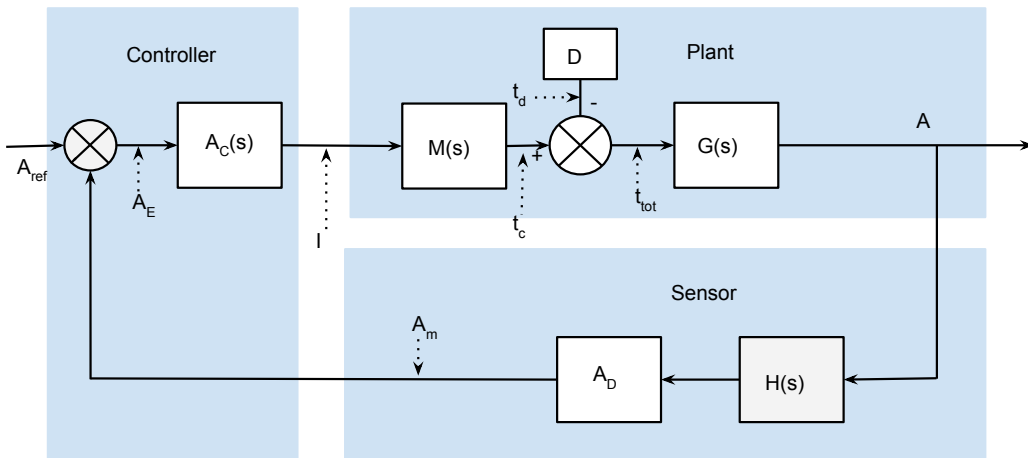


Figure 4.1: The figure shows a block diagram of the ADCS with all its different subsystems.

- $A_c(s)$ is the attitude controller.
- $M(s)$ is model of the magnetotorquers which express the relation between the magnetic torque produced be the actuators as a function of the current. This was derived in chapter 2.

- $\mathbf{D}(s)$ is the model expressing the different disturbances. This was derived in chapter 2.
- $\mathbf{G}(s)$ is the model of the satellite.
- $\mathbf{H}(s)$ is the model of the sensors expressing how the sun is orientated in relation to the satellite.
- \mathbf{A}_D is the attitude determination model which expresses how the satellite is orientated in relation to Earth.

The focus of this chapter will be to determine A_D and $G(s)$ since all other subsystems have been dealt with in chapter 2, except $A_C(s)$ which will be derived in chapter 5. The determinations will be done in the given order:

- Determination of $A_D(s)$.
- Determination of $G(s)$.

4.1 The Attitude Determination System, A_D

[Larsen, 2014][group 13gr632, 2013] This sections expresses the necessary matrices to *rotate* or convert vectors from one reference frame into another. These matrices will be based on the math describing orbital movement, which was elaborated and presented in section 2.3. To summarize, this section will deal with the following two main problems in the given order:

- Attitude Determination.
- Rotation between the different reference frames.

The attitude determination subsection will not solve the actual problem of how attitude is determined, but instead lead up to the solution, which will be handled definitely in the reference frame subsection, since it is closely linked here to.

Attitude Determination

Recall from section 2.3 in chapter 2 the SBRF and ECI Reference Frame. The SBRF expresses the orientation of the elements within the satellite, e.i. which way the camera is pointing, and the ECIRF expresses the orientation of object in relation

to Earth. The attitude of the satellite can be described as the rotation between the SBRF and the ECIRF.

Furthermore, recall from figure 4.1 that the input to the attitude determination module is the output from the sensors of the satellite, which is two vectors describing the orientation of the sun, \mathbf{s}_{sun} , and the magnetic field of the Earth, \mathbf{s}_{mag} , in relation to the satellite. The same two vectors can be found in relation to the Earth, or the ECI Reference Frame, \mathbf{i}_{sun} and \mathbf{i}_{mag} , by using the IGRF model and an ephemeris model as explained in chapter 2.

The concept of the attitude determination can be stated as followed; we want to find a matrix which explains the rotation of the vectors \mathbf{s}_{sun} and \mathbf{s}_{mag} from the SBRF into the vectors \mathbf{i}_{sun} and \mathbf{i}_{mag} in the ECI Reference Frame. By using this method though to determine the attitude, some problems or difficulties may occur. When the satellite is in eclipse the sun vector becomes unavailable, since there is no sun shining at the satellite. This problem is critical, since the system can not make an attitude estimation when the satellite is in eclipse. Therefore it is not possible with the current system to control the satellite during eclipse.

Whaba's Problem

[Whabba, n.d.] As mentioned, the goal for the attitude determination is to find a matrix which explains the rotation of the vectors \mathbf{s}_{sun} and \mathbf{s}_{mag} from the SBRF into the vectors \mathbf{i}_{sun} and \mathbf{i}_{mag} in the ECI Reference Frame. This can be done by solving *Whaba's Problem*.

Wahba's problem can be stated as a cost function, shown in equation 4.1, that one should try to minimize as much as possible.

$$J(\mathbf{R}) = \frac{1}{2} \sum_{k=1}^N \|\mathbf{w}_k - \mathbf{R}\mathbf{v}_k\|^2 \quad (4.1)$$

Where \mathbf{w}_k is a set of k vectors in one reference frame and \mathbf{v}_k is the corresponding set of vectors in the other frame. The matrix, \mathbf{R} , is describing the rotation between the two reference frames. Whaba's problem can be solved in a number of ways, here among by using the SVD (Singular Value Decomposition) method. It can be shown that Whaba's problem can be solved by finding the SVD(\mathbf{B}) where \mathbf{B} is a matrix given by equation 4.2.

$$\text{SVD}(\mathbf{B}) = \mathbf{U} \cdot \mathbf{S} \cdot \mathbf{V}^T$$

Where B is:

$$\mathbf{B} = \sum_{k=1}^n a_k \cdot \mathbf{w}_k \cdot \mathbf{v}_i^T \quad (4.2)$$

a_k in equation 4.2 is simply an optional scalar that can be used in case one set of vectors should be weighted higher than another set of vectors. Once the SVD has been determined the rotation matrix, \mathbf{R} , can be calculated by equation 4.3

$$\mathbf{R} = \mathbf{U} \cdot \mathbf{M} \cdot \mathbf{V}^T$$

Where :

$$\mathbf{M} = \text{diag} \left(\begin{bmatrix} 1 & 1 & \det(\mathbf{U}) \cdot \det(\mathbf{V}) \end{bmatrix} \right) \quad (4.3)$$

The Rotation of the Reference Frames

[Larsen, 2014] Recall from section 2.3 the different reference frames and their definition. This section derives the different rotation matrices necessary to rotate from one frame into the ECI Reference Frame. The general matrix rotation theory used in this section to setup the matrices can be studied in appendix A. The following rotations will be examined in the given order:

- Rotation Between the ECIRF and the SBRF.
- Rotation Between the ECIRF and the ORF.
- Rotation Between the ECIRF and the ECEFRF.
- Rotation Between the ECIRF and the TRF.
- Rotation Between the SBRF and the CRF.

Notice that there is no rotation between the SBRF and the ORF. This is because the goal for the entire system is to align the SBRF and the ORF. In other words, when the system knows its attitude and the relation between the different reference frames, the controller will then in the end rotate the SBRF into the ORF when it turns the satellite.

Rotation Between the ECIRF and the SBRF

As mentioned, the attitude determination can be described as the rotation between the ECIRF and the SBRF. In the attitude determination section it was explained that first step to determining will be to setup a matrix \mathbf{B} from the sensors on the satellite and the solar- and magnetic models. This is illustrated in equation 4.4.

$$\mathbf{B} = a_{k1} \cdot \mathbf{s}_{\mathbf{v}_{\text{sun}}} \cdot \mathbf{i}_{\mathbf{v}_{\text{sun}}}^T + a_{k2} \cdot \mathbf{s}_{\mathbf{v}_{\text{mag}}} \cdot \mathbf{i}_{\mathbf{v}_{\text{mag}}}^T \quad (4.4)$$

Where a_{k1} and a_{k2} are scalars used to weight either the sun vectors or the magnetic vectors more then the other. This could be useful when the satellite is eclipse and the attitude needs to be determined, but for now both scalars will be set to one. The next step will be to determine the SVD(\mathbf{B}) which consist of three matrices \mathbf{U} , \mathbf{S} and \mathbf{V}

The matrix \mathbf{U} consist of the eigenvectors of the matrix, $\mathbf{M}_u = \mathbf{B} \cdot \mathbf{B}^T$.

The matrix \mathbf{V} consist of the eigenvectors of the matrix, $\mathbf{M}_v = \mathbf{B}^T \cdot \mathbf{B}$.

The matrix \mathbf{S} consist of the square root of the eigenvalues of either \mathbf{M}_u or \mathbf{M}_v . When the SVD has been determined the rotation matrix ${}^I\mathbf{R}$ can be found with equation 4.3.

Rotation Between the ECI and the ORF

The relation between these two frames will be done using only algebra due to the reason that the data necessary to make this matrix change in time. Recall that the ORF has its Z-axis pointing in the direction of the center of the Earth and its X-axis is aligned with the velocity vector of the satellite. These two parameters can be measured in relation to Earth thereby providing the satellite with the following two vectors:

The position vector: ${}^I\mathbf{v}_{\text{sat-p}} = [\mathbf{x}_{\text{sat-p}} : \mathbf{y}_{\text{sat-p}} : \mathbf{z}_{\text{sat-p}}]$

The velocity vector: ${}^I\mathbf{v}_{\text{sat-v}} = {}^I\dot{\mathbf{v}}_{\text{sat-p}} = [\dot{\mathbf{x}}_{\text{sat-p}} : \dot{\mathbf{y}}_{\text{sat-p}} : \dot{\mathbf{z}}_{\text{sat-p}}]$.

These two vectors can be used to create a matrix that rotates elements from the ECIRF to the ORF reference frame as equation 4.5 shows.

$${}^I_O\mathbf{R} = \begin{bmatrix} {}^I_O\mathbf{x} & {}^I_O\mathbf{y} & {}^I_O\mathbf{z} \end{bmatrix} \quad (4.5)$$

Where :

$$\overset{\text{I}}{\text{O}}\mathbf{x} = \frac{1}{\sqrt{\dot{x}_{\text{sat-p}}^2 + \dot{y}_{\text{sat-p}}^2 + \dot{z}_{\text{sat-p}}^2}} \cdot \begin{bmatrix} \dot{x}_{\text{sat-p}} \\ \dot{y}_{\text{sat-p}} \\ \dot{z}_{\text{sat-p}} \end{bmatrix}$$

$$\overset{\text{I}}{\text{O}}\mathbf{z} = \frac{1}{\sqrt{x_{\text{sat-p}}^2 + y_{\text{sat-p}}^2 + z_{\text{sat-p}}^2}} \cdot \begin{bmatrix} x_{\text{sat-p}} \\ y_{\text{sat-p}} \\ z_{\text{sat-p}} \end{bmatrix}$$

$$\overset{\text{I}}{\text{O}}\mathbf{y} = \overset{\text{I}}{\text{O}}\mathbf{z} \times \overset{\text{I}}{\text{O}}\mathbf{x}$$

This matrix can then be converted into a quaternion by the theory explained in appendix A. The quaternion that rotates elements from the ORF to the ECI Reference Frame can be found by: $\overset{\text{O}}{\text{q}} = \overset{\text{I}}{\text{O}}\mathbf{q}^{-1} = \overset{\text{I}}{\text{O}}\mathbf{q}^{\text{T}*} = \mathbf{q} (\overset{\text{I}}{\text{O}}\mathbf{R})^{\text{T}*}$.

Rotation Between the ECI and ECEFRF

The rotation relation between these two reference frames is rather simple to understand. Both the ECI Reference Frame and the ECEF Reference frame share the same Z-axis, going through the geographical North pole of the Earth. This means that a rotation from the ECEFRF into the ECIRF can be described as a simple rotation around the Z-axis. A rotation around the Z-axis can be described with the direction cosine matrix shown in equation 4.6.

$$\overset{\text{E}}{\text{R}} = \begin{bmatrix} \cos(\theta) & -\sin(\theta) & 0 \\ \sin(\theta) & \cos(\theta) & 0 \\ 0 & 0 & 1 \end{bmatrix} \quad (4.6)$$

If a vector is known in the ECEF Reference Frame, the matrix in equation 4.6 can simply be multiplied with that vector in order to get the corresponding vector in the ECI Reference Frame. Equation 4.7 to 4.10 shows how the direction cosine matrix converted into a quaternion.

$$\overset{E}{I}q_4 = \frac{1}{2} \cdot (\text{Trace}(\overset{E}{I}\mathbf{R}) + 1)^{\frac{1}{2}} = \sqrt{\frac{1 + \cos(\theta)}{2}} \quad (4.7)$$

$$\overset{E}{I}q_3 = \frac{1}{4 \cdot \overset{E}{I}q_4} \cdot (\overset{E}{I}R_{12} - \overset{E}{I}R_{21}) = \frac{-\sin(\theta)}{\sqrt{2 + 2 \cdot \cos(\theta)}} \quad (4.8)$$

$$\overset{E}{I}q_2 = \frac{1}{4 \cdot \overset{E}{I}q_4} \cdot (\overset{E}{I}R_{31} - \overset{E}{I}R_{13}) = 0 \quad (4.9)$$

$$\overset{E}{I}q_1 = \frac{1}{4 \cdot \overset{E}{I}q_4} \cdot (\overset{E}{I}R_{23} - \overset{E}{I}R_{32}) = 0 \quad (4.10)$$

The angle θ depends on the time since the last vernal equinox. The ECEFRF and the ECIRF are aligned once on every rotation of the Earth. This takes 23 hours, 56 minutes and 4 second, corresponding to every 8616409053 seconds. With that information the angle can be calculated with equation 4.11, where τ is the orbit time.

$$\theta = 2 \cdot \pi \cdot \frac{\tau}{8616409053} \quad (4.11)$$

Furthermore, notice that $\overset{I}{E}\mathbf{q} = \overset{E}{I}\mathbf{q}^{-1} = \overset{I}{E}\mathbf{q}^{T*}$.

Rotation Between the ECI and TRF

The method for finding this rotation matrix is very similar to that of the ORF into the ECI Reference Frame. The TRF is especially important when the satellite is set to point at AAU. Recall that the Z-axis of the TRF points at AAU. The position of AAU within the ECEFRF is 3427961, 603674, 5326755. This point or location needs to be rotated into the ECI Reference Frame using either $\overset{E}{I}\mathbf{R}$ or $\overset{E}{I}\mathbf{q}$. Consider the vector $\overset{I}{v}_{AAU}$ which goes from the center of the Earth to AAU. The rotation matrix, $\overset{I}{T}\mathbf{R}$, can be found with equation 4.12.

$$\overset{I}{T}\mathbf{R} = \begin{bmatrix} \overset{I}{T}\mathbf{x} & \overset{I}{T}\mathbf{y} & \overset{I}{T}\mathbf{z} \end{bmatrix} \quad (4.12)$$

Where :

$$\frac{\mathbf{I}_{\mathbf{T}} \mathbf{z}}{\|\mathbf{I}_{\mathbf{T}} \mathbf{z}\|} = \frac{\mathbf{I}_{\mathbf{v}_{\text{sat-p}}} - \mathbf{I}_{\mathbf{v}_{\text{AAU}}}}{\|\mathbf{I}_{\mathbf{v}_{\text{sat-p}}} - \mathbf{I}_{\mathbf{v}_{\text{AAU}}}\|}$$

$$\begin{aligned}\frac{\mathbf{I}_{\mathbf{T}} \mathbf{y}}{\|\mathbf{I}_{\mathbf{T}} \mathbf{y}\|} &= \frac{\mathbf{I}_{\mathbf{v}_{\text{sat-p}}}}{\|\mathbf{I}_{\mathbf{v}_{\text{sat-p}}}\|} \\ \frac{\mathbf{I}_{\mathbf{T}} \mathbf{x}}{\|\mathbf{I}_{\mathbf{T}} \mathbf{x}\|} &= \frac{\mathbf{I}_{\mathbf{T}} \mathbf{z}}{\|\mathbf{I}_{\mathbf{T}} \mathbf{z}\|}\end{aligned}$$

This matrix can then be converted into a quaternion by the theory explained in appendix A. The quaternion that rotates elements from the TRF to the ECI Reference Frame can be found by: $\frac{\mathbf{T}}{\mathbf{I}} \mathbf{q} = \frac{\mathbf{I}}{\mathbf{T}} \mathbf{q}^{-1} = \frac{\mathbf{I}}{\mathbf{T}} \mathbf{q}^{\text{T}*} = \mathbf{q} (\frac{\mathbf{I}}{\mathbf{T}} \mathbf{R})^{\text{T}*}$.

Rotation Between the SBRF and CRF

The controller regulates the satellite in the CRF. When the controller has produced a control signal, this need to be rotated into the SBRF before being send into magnetorquers. This reference frame always has the same orientation relative to the SBRF and therefore the controller calculations dependent only on the moment of inertia and the definition of CRF. It is determined that the axis of the CRF are set as principal axes of the satellite defined by the inertia, which makes the inertia matrix in the CRF into a diagonal matrix. By applying the EVD (Eigen Value Decomposition) to the inertia matrix in the SBRF a matrix that diagonalises the inertia matrix can be found.

The EVD of a matrix is simply a matrix that consist of the eigenvectors of that matrix. The rotation matrix $\frac{\mathbf{C}}{\mathbf{S}} \mathbf{R}$ is given by equation 4.13.

$$\frac{\mathbf{C}}{\mathbf{S}} \mathbf{R} = \begin{bmatrix} 0.9821 & 0.1666 & 0.0881 \\ 0.1170 & 0.9055 & 0.4078 \\ 0.1477 & 0.3902 & 0.9088 \end{bmatrix} \quad (4.13)$$

As with all other rotation matrices this matrix can also be re-written into a quaternion, given by equation 4.14 to 4.17.

$${}_{\text{S}}^{\text{C}} \mathbf{q}_4 = \frac{1}{2} \cdot (\text{Trace}({}_{\text{S}}^{\text{C}} \mathbf{R}) + 1)^{\frac{1}{2}} = \frac{1}{2} \sqrt{1 + {}_{\text{S}}^{\text{C}} R_{11} + {}_{\text{S}}^{\text{C}} R_{22} + {}_{\text{S}}^{\text{C}} R_{33}} = 0.9744 \quad (4.14)$$

$${}_{\text{S}}^{\text{C}} \mathbf{q}_3 = \frac{1}{4 \cdot {}_{\text{S}}^{\text{C}} \mathbf{q}_4} \cdot ({}_{\text{S}}^{\text{C}} R_{12} - {}_{\text{S}}^{\text{C}} R_{21}) = 0.0727 \quad (4.15)$$

$${}_{\text{S}}^{\text{C}} \mathbf{q}_2 = \frac{1}{4 \cdot {}_{\text{S}}^{\text{C}} \mathbf{q}_4} \cdot ({}_{\text{S}}^{\text{C}} R_{31} - {}_{\text{S}}^{\text{C}} R_{13}) = -0.0606 \quad (4.16)$$

$${}_{\text{S}}^{\text{C}} \mathbf{q}_1 = \frac{1}{4 \cdot {}_{\text{S}}^{\text{C}} \mathbf{q}_4} \cdot ({}_{\text{S}}^{\text{C}} R_{23} - {}_{\text{S}}^{\text{C}} R_{32}) = -0.2039 \quad (4.17)$$

4.2 Model of the Satellite, $G(s)$

In this section the mathematical models of the satellite will be derived, to get a understanding of the satellites behaviour in space. This is done by a kinematic model describing how the satellite acts upon a torque in space and by a dynamic model describing the torques that act upon the satellite. These models are then used for designing the control algorithm to give the correct attitude control of the satellite and later to test the functionality of the control algorithm.

Kinematic Model of the Satellite

[Wertz, 1999] The kinematic model of the satellite is used for attitude propagation. Attitude propagation of the spacecraft is based on present angular velocity and measured attitude in conjunction with the kinematic equations describing the satellite. The kinematic equations describe the time dependant rotation of the satellite.

This rotation can be described by a quaternion $\mathbf{q}(t)$ which changes in time. This quaternion can be described by a double rotation, from the last known position of the SBRF to the ECIRF and a quaternion $\mathbf{q}(\Delta t)$ which describes the rotation since time t . These two can be multiplied together to give $\mathbf{q}(t+\Delta t)$ which is a multiplication of the complete rotation of $\mathbf{q}(t)$ and $\mathbf{q}(\Delta t)$. The elements in $\mathbf{q}(\Delta t)$ consists of

$$\begin{aligned} q(\Delta t)_1 &= e_x \sin \frac{\Delta \Phi}{2} \\ q(\Delta t)_2 &= e_y \sin \frac{\Delta \Phi}{2} \\ q(\Delta t)_3 &= e_z \sin \frac{\Delta \Phi}{2} \\ q(\Delta t)_4 &= \cos \frac{\Delta \Phi}{2} \end{aligned}$$

Where: e_u, e_v, e_w are the components of the euler eigenaxis as unit vectors along SBRF at time t . $\Delta\Phi$ is the rotation at time $q(\Delta t)$. The complete rotation after Δt can be expressed as the multiplication of the two quaternions.

$$q(t + \Delta t) = q(\Delta t)q(t) \quad (4.18)$$

This can also be written on matrix form where the composition of the skew symmetry matrix holding the components of $q(\Delta t)$ is obtained from quaternion multiplication and I is the identity matrix.

$$q(\Delta t) = \cos \frac{\Delta\Phi}{2} I_{4x4} + \sin \frac{\Delta\Phi}{2} \begin{bmatrix} 0 & e_z & -e_y & e_x \\ -e_z & 0 & e_x & e_y \\ e_y & -e_x & 0 & e_x \\ -e_x & -e_z & -e_y & 0 \end{bmatrix} \quad (4.19)$$

This can be written as a differential equation where the time Δt is infinitesimal and the angle $\Delta\Phi = \omega\Delta t$. When the time is infinitesimal the angle becomes very small, approximations can be made for sine and cosine.

$$\sin \frac{\Delta\Phi}{2} \approx \frac{1}{2}\omega\Delta t \quad \cos \frac{\Delta\Phi}{2} \approx 1 \quad (4.20)$$

Equation 4.19 can then be simplified to:

$$q(\Delta t) = [I + \frac{1}{2}\Omega\Delta t]q(t) \quad (4.21)$$

Where Ω is the skew symmetry matrix and $\omega = \omega\hat{e}$ is the angular velocity along the eigenaxis.

$$\Omega = \begin{bmatrix} 0 & \omega_z & -\omega_y & \omega_x \\ -\omega_z & 0 & \omega_x & \omega_y \\ \omega_y & -\omega_x & 0 & \omega_x \\ -\omega_x & -\omega_z & -\omega_y & 0 \end{bmatrix} \quad (4.22)$$

The derivative of 4.21 can be found as:

$$\frac{dq}{dt} \equiv \lim_{\Delta t \rightarrow 0} \frac{q(t + \Delta t) - q(t)}{\Delta t} = \lim_{\Delta t \rightarrow 0} \frac{q(t) + \frac{1}{2}\Omega q(t) - q(t)}{\Delta t} = \frac{1}{2}\Omega q \quad (4.23)$$

In this equation the time, Δt should be kept sufficiently small so that ω is kept constant over the duration. When this is the case, 4.23 can be integrated to give the solution of the rotation over time.

$$q(t) = e^{\frac{1}{2}\Omega q(t)} q(0) \quad (4.24)$$

The exponential function of a matrix is the equivalent of a series of sines and cosines which can be written out to:

$$e^{\frac{1}{2}\Omega q(t)} q(0) = \cos \frac{\omega t}{2} I_{4 \times 4} + \sin \frac{\omega t}{2} \begin{bmatrix} 0 & e_z & -e_y & e_x \\ -e_z & 0 & e_x & e_y \\ e_y & -e_x & 0 & e_x \\ -e_x & -e_z & -e_y & 0 \end{bmatrix} q(0) \quad (4.25)$$

It is seen that the end result is the same as in 4.19 and therefore the quaternion obtained through this process gives the correct attitude propagation over time.

Dynamic Model of the Satellite

To describe the relation between a force, F , exerted on a body and the translational motion of the body in terms of its acceleration, a , and its mass, m , Newton's second law is used:

$$F(t) = m \cdot a(t) \quad (4.26)$$

Equation 4.26 is disregarding any friction. Since the satellite is a rotation body a look upon the counterpart to Equation 4.26 would be desirable. Exerted on the body is a torque, τ , to the motion of the body in terms of its acceleration, α , and inertia, J :

$$\tau(t) = J \cdot \alpha(t) \quad (4.27)$$

Just as Equation 4.26, Equation 4.27 is also disregarding any friction.

Moment of inertia

The torque needed for a desired angular acceleration about an axis of rotation is defined by the mass property of a rigid body, called the moment of inertia. The torque for acceleration or deceleration of a body varies depending on the shape. But considering a point mass where the moment of inertia is defined relative to the center of the mass, the equation can be described as:

$$J = \sum_{i=1}^n m_i \cdot r_i^2 \quad (4.28)$$

where:

J is the moment of inertia of the body

m_i is the mass of the i^{th} particle

r_i^2 is the distance from the rotational axis to the i^{th} particle

Since the rotational axis can be any axis going through the center of the body, *Steiners theorem* is used to find the inertia of the body's center of mass. Steiners theorem can be explained by stating an example with a body that is rotating about an axis z , where the z axis is passing through the body's center of mass. This body contains a moment of inertia with respect to the z axis, e.i. going through the body's center of mass. Steiners theorem then states, that if the body were made to rotate about another axis z' , parallel to the z axis, then the moment of inertia of the z -axis could be displayed as:

$$J = J_{cm} + M \cdot r^2 \quad (4.29)$$

where:

J is the moment of inertia of the z -axis

J_{cm} is the moment of inertia around the z axis, going through the center of mass

M is the object's mass

r is the distance between the two parallel axes

This does only comply to objects fixed in a single axis, since the the satellite is a body able to move in a three dimensional space, the inertia will be expressed as a matrix. The inertia is expressed as the matrix $s\bar{J}$ in the SBRF:

$$\mathbf{J} = \begin{bmatrix} I_{xx} & -I_{xy} & -I_{xz} \\ -I_{yx} & I_{yy} & -I_{yz} \\ -I_{zx} & -I_{zy} & I_{zz} \end{bmatrix} \quad (4.30)$$

The inertia matrix will be a diagonal matrix, if the rigid body is symmetrical in all axes, and if the diagonal is zero, then when a constant torque is applied the body would get an infinite angular velocity, if the torque is applied over an infinitely long period of time. The inertia matrix for the satellite is given by a 3D computer model made in *Inventor*. Equation 4.31 illustrates the inertia matrix. In an attempt to verify this inertia matrix the first value of the matrix, $4806 \cdot 10^{-6}$ kg · m², has been measured. This experiment can be found in appendix C.

$${}^S\mathbf{J} = \begin{bmatrix} 4806.218 & 10636.223 & 13438.362 \\ 10636.223 & 92852.250 & 1627.530 \\ 13438.362 & 1627.530 & 92147.773 \end{bmatrix} \cdot 10^{-6} \quad [\text{kg} \cdot \text{m}^2] \quad (4.31)$$

In section 4.1 it was determined that the axis of the CRF are principal axes of the satellite defined by the inertia, and hence the inertia matrix in the CRF becomes a diagonal matrix. Recall from that section the rotation matrix ${}^C_S\mathbf{R}$ given by equation 4.32.

$${}^C_S\mathbf{R} = \begin{bmatrix} 0.9821 & 0.1666 & 0.0881 \\ 0.1170 & 0.9055 & 0.4078 \\ 0.1477 & 0.3902 & 0.9088 \end{bmatrix} \quad (4.32)$$

The inertia matrix in the control reference frame can be found by equation 4.34.

$${}^S\mathbf{J} = {}^C_S\mathbf{R} \cdot {}^C\mathbf{J} \cdot {}^S_C\mathbf{R}^{-1} \quad (4.33)$$

\Leftrightarrow

$${}^C\mathbf{J} = \begin{bmatrix} 1518 & 0 & 0 \\ 0 & 94107 & 0 \\ 0 & 0 & 94108 \end{bmatrix} \cdot 10^{-6} \quad [\text{kg} \cdot \text{m}^2] \quad (4.34)$$

The inertia matrix in equation 4.34 is the one that will be used later on in the design of the controller since all regulation takes place in the CRF.

Dynamic equation of the satellite

When talking about dynamic equations of the satellite, it is essential to mention and explain angular momentum, as it gives the opportunity to describe all torques affecting the rotating body in space. Attitude dynamics is evaluated in an inertial reference frame, and relates the angular velocity of a rigid body, relative to its center of mass. The angular momentum is expressed by:

$$\mathbf{L}_{\text{tot}} = \sum_{i=1}^n \mathbf{r}_i \times \mathbf{P}_i = \sum_{i=1}^n \mathbf{r}_i \times m_i \mathbf{v}_i \quad (4.35)$$

where:

L_{tot} is the angular momentum of the rigid body

r_i is the position of the i^{th} point mass in inertial space

P_i is the momentum of the i^{th} point mass

m_i is the mass of the i^{th} point mass

v_i is the translational velocity of the i^{th} point mass

From Equation 4.35 it is possible to find an equation for the total external torque. This is simply done by differentiating Equation 4.35 with respect to time:

$$\frac{d\mathbf{L}_{\text{tot}}}{dt} = \sum_{i=1}^n \frac{d}{dt} (\mathbf{r}_i \times m_i \mathbf{v}_i) \quad (4.36)$$

$$= \sum_{i=1}^n (\mathbf{v}_i \times m_i \mathbf{v}_i + \mathbf{r}_i \times m_i \mathbf{a}_i) \quad (4.37)$$

$$= \sum_{i=1}^n \mathbf{r}_i \times \mathbf{F}_i \quad (4.38)$$

$$= \sum_{i=1}^n \tau_i \quad (4.39)$$

$$= \tau_{\text{tot}} \quad (4.40)$$

where:

v_i is the translational velocity, equal to the time derivative of r_i

a_i is the translational acceleration, equal to the time derivative of v_i

F_i is the force exerted on the i^{th} point mass

τ_i is the torque exerted on the i^{th} point mass

τ_{tot} is the total external torque

The internal torques sum to zero, and this results in Equation 4.40 yields the total external torque, τ_{tot} . There are two kinds of external torques contained within τ_{tot} though. These are the disturbance torque, τ_d , and the control torque, τ_c . The disturbance torques are caused by environmental effects such as the earth's magnitude and solar radiation pressure, whereas the control torque is attached jets, magnetic coils and likewise. This projects uses magnetic coils, so these will be affecting the control torque and have been explained in Section 2.1.

Complete satellite model

A complete model of the torques affecting the satellite can now be assembled, combining control torque and disturbance torques, together with the torque of the satellite. The magnitude of the disturbance torques are as mentioned in chapter 2, where the aerodynamic torque is the largest by far, and thus the only one used in later models. The complete torque model of the satellite can be expressed as:

$$\tau_{tot} = \tau_{sat} + \tau_d + \tau_c \quad (4.41)$$

$${}^c\mathbf{J} \cdot {}^c\dot{\omega}(t) = -{}^c\omega(t) \times {}^c\mathbf{J} \cdot {}^c\omega(t) + \tau_d + \tau_c \quad (4.42)$$

4.3 Summary

In this chapter the dynamic equation and kinematic models of the satellite have been described. Also the inertia matrix has been found and described and used for defining the CRF. This gives a complete description of the satellite which can be used in conjunction with the other findings in previous chapters. With this a complete model of the whole system will be made in the next chapter, and for this the controller will be designed.

Chapter 5

Design of the ACS Controller, $A_C(s)$

This chapter documents and explains the design of ACS controller, which is illustrated on figure 5.1. To summarize from previous chapters, the goal of the ACS is to align the SBRF with either the TRF or the ORF in order to acquire a decried orientation of the satellite. When it is desired to point at AAU the TRF is used, e.i. if a transmission should be done, and the ORF when the satellite should point directly on Earth, for instance when travelling or taking a picture if the satellite is provided with a camera.

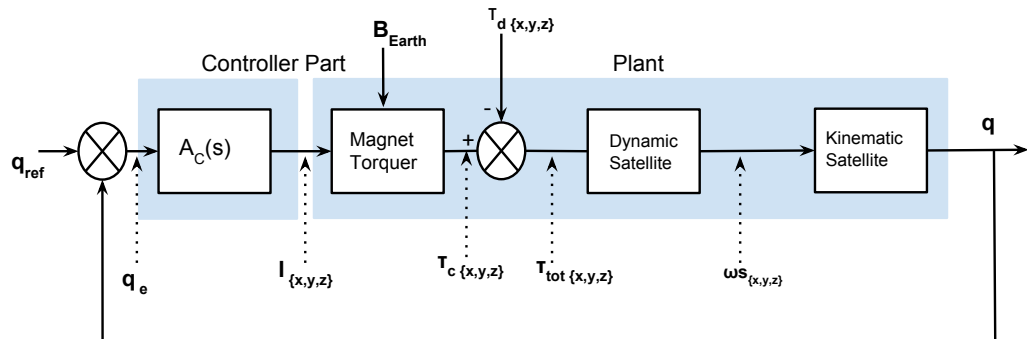


Figure 5.1: The figure shows an overview of the ACS with its different elements.

The design of the controller is based on the mathematical models described in the previous chapters. The chapter is divided into six parts which will be gone through

in the given order:

- Requirements of the controller.
- System Analysis.
- Design of the controller in Laplace Domain.
- Verification of the controller.
- Design- and Controller Corrections.
- Design of the Controller in Z-Domain.

The goal of the six parts is to give a good overview of the design procedure starting from the requirements to the system, the actual design and finally a verification and implementation of the controller.

5.1 Requirements

The focus of this section will be to setup a number of specifications for the controller, in order to be able to design and, in the end, verify its functionality. To start with, recall from chapter 3 the following requirement for the ACS controller:

- The ADCS should have a pointing precision of minimum 12° .

In order to satisfy this demand it has been decided to specify that the system should be a system type of type 1 in order to eliminate any position steady-state error.

Furthermore, it has been decided that the maximum overshoot should be, $M_P = 8\%$, because 15° corresponds to approximately 8% of 180° . This provides us with a further requirement, namely a damping factor value of $\zeta = 0.62$

As it is stated in the requirements chapter 3 the satellite is over an area for about 60 seconds where it is acceptable to take a picture. As it is wanted to have sufficient time to take the picture it has been decided to set the settling time to half of that, which is 30 seconds. This means that there is a gap of approximately 20 seconds left for the rise time.

5.2 System Analysis

This section examines the behaviour of the ACS, without the controller, in order to determine which controller should be designed. In other words, this section examines the number and behaviour of the poles in the regulation system etc. To start with, it is necessary to simplify the block diagram from figure 5.1 into the one shown in figure 5.2.

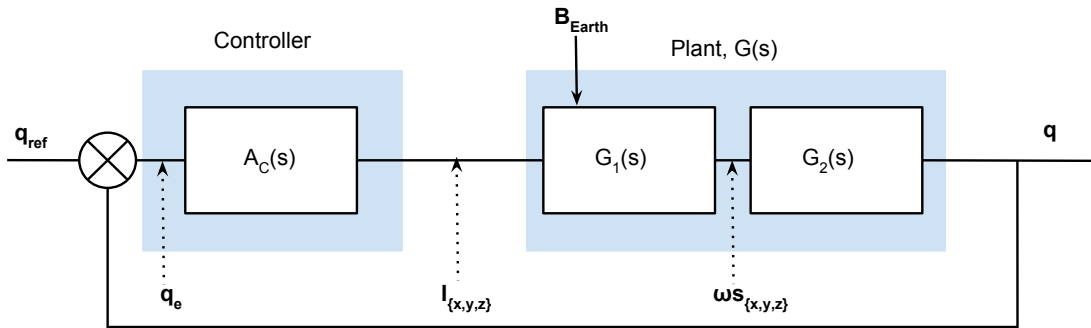


Figure 5.2: The figure shows simplification of the digram in figure 5.1.

The goal is to determine the transfer function $G(s)$ shown in figure 5.2, where $G_1(s)$ represents the combination of the magnet torquer transfer function, the summation of the different torques and the dynamic model of the satellite, shown in figure 5.1. $G_2(s)$ represents the kinematic model of the satellite.

Determination of $G(s)$

Recall from the previous chapter the dynamic model of the satellite shown in equation 5.1 and the transfer function of the magnet torquer shown in equation 5.2. Note that both equations have been Laplace transformed and are written in matrix/vector form.

$$\mathbf{J} \cdot \omega(\mathbf{s}) \cdot \mathbf{s} = (-\omega(\mathbf{s}) \times \mathbf{J} \cdot \omega(\mathbf{s})) + \tau_c + \tau_d \quad (5.1)$$

$$\tau_c(\mathbf{s}) = \mathbf{N} \cdot \mathbf{A} \cdot \mathbf{I}(\mathbf{s}) \times \mathbf{b}_{\text{earth}} \quad (5.2)$$

If it is assumed that the regulation strategy is for the system to follow the reference and not to minimize the disturbances, then $\tau_d = 0$ and with the help from figure 5.1 it is seen that equation 5.1 and 5.2 can be combined into equation 5.3 giving $G_1(s)$.

$$G_1(s) = \mathbf{J} \cdot \boldsymbol{\omega}(s) \cdot s = (-\boldsymbol{\omega}(s) \times \mathbf{J} \cdot \boldsymbol{\omega}(s)) + (\mathbf{N} \cdot \mathbf{A} \cdot \mathbf{I}(s) \times \mathbf{b}_{\text{earth}}) \quad (5.3)$$

Furthermore, recall the kinematic model of the satellite stated in equation 5.4. Note that this equation has been Laplace transformed.

$$G_2(s) = \mathbf{q}(s) = \frac{1}{s - \frac{1}{2} \cdot \boldsymbol{\Omega}} \quad (5.4)$$

Where the term $\boldsymbol{\Omega}$ is given by equation 5.5.

$$\boldsymbol{\Omega} = \begin{bmatrix} 0 & \omega_z & -\omega_y & \omega_x \\ -\omega_z & 0 & \omega_x & \omega_y \\ \omega_y & -\omega_x & 0 & \omega_z \\ -\omega_x & -\omega_y & -\omega_z & 0 \end{bmatrix} \quad (5.5)$$

Equation 5.3 and 5.4 can now be used to express the entire plant. This is done easiest by setting up a block diagram as shown in figure 5.3 to give an overview of how the behaviour. This figure shows the first of many regulation difficulty that needs to be taken care of. It is seen that the angular velocity of the satellite is *feed-backed* as an input to the block G_1 .

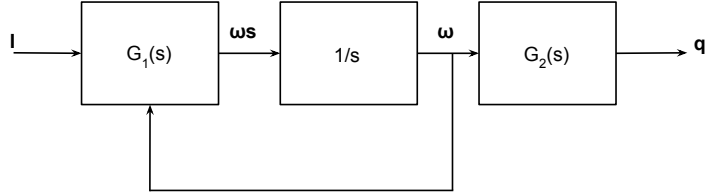


Figure 5.3: The figure shows a block diagram of the entire plant, satellite models, magnet torquers combined.

This might cause problems in the form of cross contributions between the different axis, and it is even more critical to examine how much this extra input affects the output of the block compared to the *real* input. In order to accomplish this task it is necessary to expand equation 5.3. If the satellite rotates so fast that it has not moved too far from its starting position, then it can be assumed that the contribution from

the magnetic field is rather constant. With the help from the IGRF-MATLAB script, the magnetic field above Aalborg has been determined and based on the previous assumption, equation 5.3 can be rewritten into equation 5.6.

$$\begin{bmatrix} 0.00150 \cdot \omega_x \cdot s - 7.40 \cdot 10^{-5} \cdot \omega_y \cdot \omega_z \\ 0.0941 \cdot \omega_y \cdot s + 0.0927 \cdot \omega_x \cdot \omega_z \\ 0.0942 \cdot \omega_z \cdot s - 0.0926 \cdot \omega_x \cdot \omega_y \end{bmatrix} = \begin{bmatrix} 6.17 \cdot 10^{-5} I_y - 4.30 \cdot 10^{-7} \cdot I_z \\ 2.17 \cdot 10^{-5} I_z - 6.17 \cdot 10^{-5} \cdot I_x \\ 4.30 \cdot 10^{-7} I_x - 2.17 \cdot 10^{-5} \cdot I_y \end{bmatrix} \quad (5.6)$$

Two things should be noticed in equation 5.6. Firstly, the contribution of ω_y and ω_z to the total angular acceleration is very small compared to the contribution of ω_x , which is good. Unfortunately, this is not the case of the two remaining axis. The contribution done by ω_x and ω_z to the Y-axis and ω_x and ω_y to the Z-axis, is almost the same as the contribution from ω_y and ω_z to each axis.

The cross contributions on the Y- and Z-axis can cause huge irregularities between theory and real life, depending on how they are handled. Unfortunately, since we at this level, lack the ideal tools to solve a regulation problem like this, it has been decided to assume that all cross contributions are zero in order to simplify the regulation a bit. This is of course far from the case in real life, as just proved, thereby making the controller inaccurate compared to real life behaviour. This inaccuracy will appear in some simulation and will be considered when the controller is evaluated.

Secondly, one should notice that the control signal to each axis from the controller to the plant, e.i. the current, consist of the signals of the two remaining axis. In other words, the control signal to the X-axis of the plant is a combination of the Y- and Z-axis signal and so on. This information will be come in handy when designing and implementing the controller in a simulation environment or in a real life test.

Based on these assumptions, equation 5.3 can now be rewritten into equation 5.7.

$$\begin{bmatrix} 0.00150 \cdot \omega_x \cdot s \\ 0.0941 \cdot \omega_y \cdot s \\ 0.0942 \cdot \omega_z \cdot s \end{bmatrix} = \begin{bmatrix} 6.18 \cdot 10^{-5} I_y \\ 2.18 \cdot 10^{-5} I_z \\ 4.30 \cdot 10^{-7} I_x \end{bmatrix} \quad (5.7)$$

If the integrator term from figure 5.3 is included, equation 5.7 can be turned into equation 5.8.

$$\begin{bmatrix} 0.00150 \cdot \omega_x \\ 0.0941 \cdot \omega_y \\ 0.0942 \cdot \omega_z \end{bmatrix} = \begin{bmatrix} \frac{6.18 \cdot 10^{-5}}{s} \cdot I_y \\ \frac{2.17 \cdot 10^{-5}}{s} \cdot I_z \\ \frac{4.30 \cdot 10^{-7}}{s} \cdot I_x \end{bmatrix} \quad (5.8)$$

The last part shown in figure 5.3, the kinematic model of the satellite described by equation 5.4, can be simplified into a simple integration term because it was assumed that all the cross contributions are zero and since the diagonal of the matrix $[\omega] \otimes R$ is zero as well, the remaining part of equation 5.4 is an integration. Thereby, equation 5.8 can be rewritten into equation 5.9 giving $G(s)$.

$$G_{x,y,z}(s) = \frac{\Theta_{x,y,z}}{I_{x,y,z}} = \begin{bmatrix} \frac{\Theta_x}{I_y} \\ \frac{\Theta_y}{I_z} \\ \frac{\Theta_z}{I_x} \end{bmatrix} = \begin{bmatrix} \frac{6.18 \cdot 10^{-5}}{0.00150 \cdot s^2} \\ \frac{2.17 \cdot 10^{-5}}{0.0941 \cdot s^2} \\ \frac{4.30 \cdot 10^{-7}}{0.0942 \cdot s^2} \end{bmatrix} \quad (5.9)$$

Analysis of $G(s)$

Equation 5.9 can be divided into equation 5.10 to 5.12 describing the behaviour of the entire plant in the X-, Y- and Z-axis.

$$G_x(s) = \frac{6.18 \cdot 10^{-5}}{1.53 \cdot 10^{-3} \cdot s^2} = \frac{0.0404}{s^2} \quad (5.10)$$

$$G_y(s) = \frac{2.17 \cdot 10^{-5}}{0.0941 \cdot s^2} = \frac{2.31 \cdot 10^{-4}}{s^2} \quad (5.11)$$

$$G_z(s) = \frac{4.30 \cdot 10^{-7}}{0.0942 \cdot s^2} = \frac{4.67 \cdot 10^{-7}}{s^2} \quad (5.12)$$

It is seen that the transfer functions in equation 5.10 to 5.12 each have a second order pole in zero. It may seem odd at first that each axis have exactly the same pole locations, but considering that it is the same coil affecting the plant in each direction, the number of poles and their location is very logical.

The figure 5.4 shows the step response of the transfer function $G_x(s)$. The step responses for the two other axis can be seen in appendix D. From figure 5.4 it is clearly seen that the system is very unstable, which is no surprise due to a second order pole in zero and nothing more.

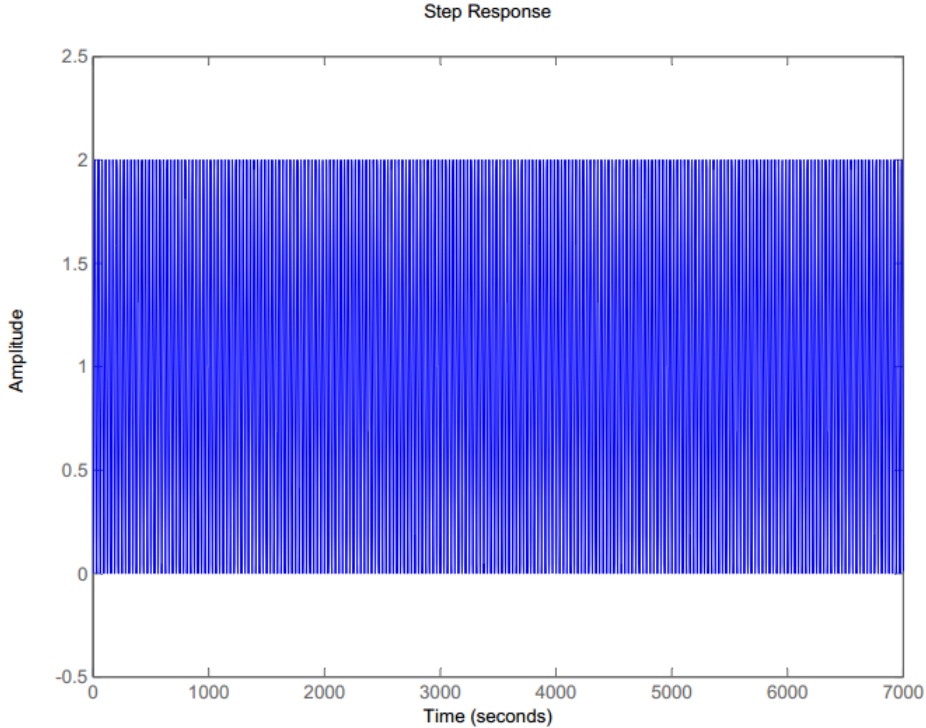


Figure 5.4: The figure shows a step response to the X-axis transfer function without a controller.

The main goal of the controller will, first of all, be to make the system stable, hence it has been chosen to design the controller as a LEAD-compensation. This controller type moves the pole to the left thereby increasing the responsiveness and stability of the system. The LEAD-compensation is a modification of the PD-controller. When the system has become stable, the P-controller will provide the system with a desired rise time. Furthermore, D-controller will both improve system speed (settling time), but also suppress some the overshoot caused by the P-controller, thereby keeping the system under the 8% overshoot limit.

5.3 Design of the Controller in the Laplace Domain

This section focuses on the design of actual controller. As mentioned in the analysis section it has been decided to use a LEAD-compensation, which in its general form is illustrated by equation 5.13.

$$A_c(s) = K \cdot \frac{s + z}{s + p} \quad (5.13)$$

The damping and settling time requirements to the system, $\zeta = 0.62$ and $\tau_s \leq 30s$, can be used to determine the minimum natural undamped frequency, $\omega_n = 0.62$, of the system illustrated by equation 5.14.

$$\tau_s = \frac{4.6}{\zeta \cdot \omega_n} \Leftrightarrow \omega_n = \frac{4.6}{\zeta \cdot \tau_s} = \frac{4.6}{0.62 \cdot 30 s} = 0.255 \text{ rad/s} \quad (5.14)$$

Provided this information the limit location of the dominant pole, P_0 , can be determined using that $\omega_n = r$ and $\theta_p = \sin^{-1}(\zeta)$. P_0 is shown in equation 5.15.

$$P_0 = r \cdot e^{\theta_p} = 0.225 \cdot e^{36.87^\circ} = -0.166 + 0.2 \cdot j \quad (5.15)$$

A good *design rule* when designing a LEAD-compensation is to choose the placement of the pole such that it is 5 to 20 times greater than the zero. This is done to minimize the effect of the pole in relation to the zero also added by the LEAD-compensation. To start with the pole is set at approximately $p = -30$. Figure 5.5 shows the location of all the poles from the system and the controller.

The location of zero added by the LEAD-compensation can be determined by using figure 5.5 and the two equations 5.16 and 5.17.

$$\begin{aligned} \psi - \theta_1 - \theta_2 &= 180^\circ \Leftrightarrow \psi = 180^\circ + \theta_1 + \theta_2 \\ &= 180^\circ + 128.87^\circ \cdot 2 + 3^\circ \\ &= 440.74^\circ \Rightarrow 80.74^\circ \end{aligned} \quad (5.16)$$

$$z = -\frac{\|P_0\|}{\sin(\psi)} \cdot \sin(\theta_p) = -\frac{0.255}{\sin(80.74^\circ)} \cdot \sin(128.87^\circ) = -4.87 \quad (5.17)$$

Now that the pole and zero location of the LEAD-controller has been determined the only missing parameter in the controller is the gain, K . The gain determine the actual location of the dominant pole, so the goal is to find a K value that provides a pole with the same ζ value as P_0 and an ω_n value larger or equal to that of P_0 . To

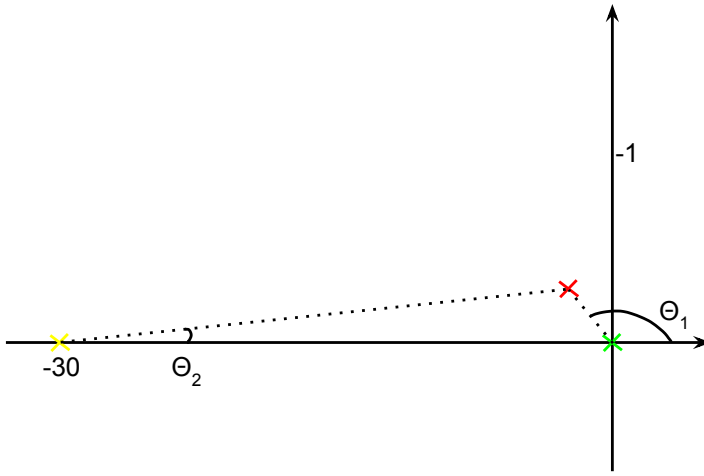


Figure 5.5: The figure a pole/zero map of the entire system. The green pole is from the plant, the red pole is the dominant pole set by the requirement and the yellow pole is from the LEAD-compensation.

find a satisfying value of the gain, the root locus of the system has been determined and plotted. Figure 5.6 shows the root locus of the X-axis of system.

It is seen from figure 5.6 that the root locus passes through the $\zeta = 0.62$ asymptote thereby providing a gain of $K_x = 6.61 \cdot 10^3$ to the X-axis controller. It is furthermore seen from the root locus that the system is generally stable, no poles are located or moving into the right half plane. The same analysis is done for the Y- and Z-axis resulting in the three controllers shown in equation 5.18 to 5.20. The root locus of the Y- and Z-axis can be seen in appendix D.

$$A_{cx}(s) = K_x \cdot \frac{s + z}{s + p} = 6.61 \cdot 10^3 \cdot \frac{s + 4.87}{s + 30} \quad (5.18)$$

$$A_{cy}(s) = K_y \cdot \frac{s + z}{s + p} = 1.15 \cdot 10^6 \cdot \frac{s + 4.87}{s + 30} \quad (5.19)$$

$$A_{cz}(s) = K_z \cdot \frac{s + z}{s + p} = 5.71 \cdot 10^8 \cdot \frac{s + 4.87}{s + 30} \quad (5.20)$$

It is seen that the gain in the controllers are very high. But this is explained by the very high damping that is seen in the description of the satellite. Because the orders of magnitude of the controller gain cancels out with the orders of magnitude on the damping, this means that the relative gain is not alarmingly high.

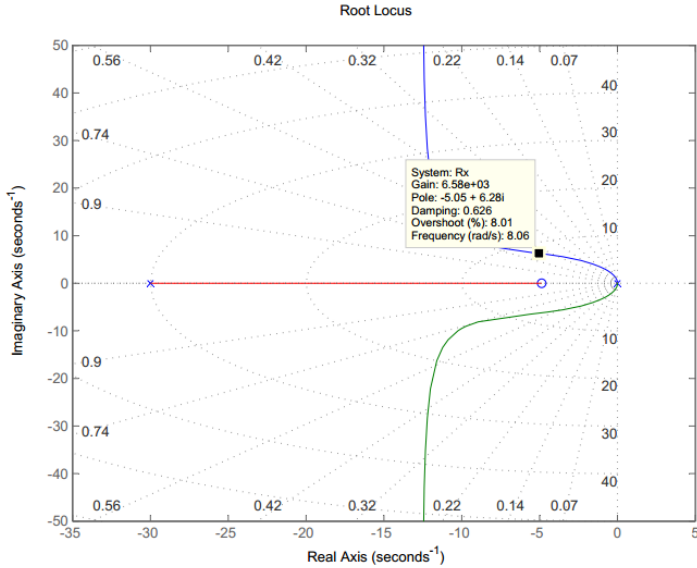


Figure 5.6: The figures the root locus of the poles and zeros in the X-axis transfer function along with the poles and zeros from the X-axis controller

5.4 Verification of the Controller

The goal of this section is verify the controllers according to the requirement specified in the beginning of the chapter. The verification will only be done for one controller, the verification of the two remaining controllers will be done in appendix D. Figure 5.7 shows the step response of the X-axis system.

It seen from figure 5.7 that there is no steady-state error. The settling time is much less than the requirement of 30 s and the overshoot is not above 8%. Based on this result it can be concluded that the controller works as designed to.

5.5 Design- and Controller Corrections (Feed-Forward)

One of the assumption made in the design of the controller was to assume that the disturbance torque, $\tau_d = 0$. As shown in chapter 2 this is far from the truth. The focus of this section will be to evaluate the functionality of the controller along with the disturbances in outer space.

In chapter 2 it was shown that the disturbance torque mainly consisted of the aerodynamic drag, which was constant. The fact that this disturbance is constant is very important, because it allows the use of a technique *Forward-Feedback* or *Feed-Forward*. This is a very popular technique used to minimize the effect of disturbances

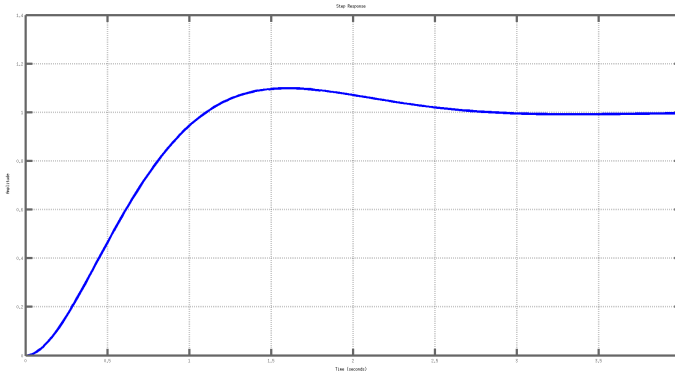


Figure 5.7: The figures the step response of the X-axis system, the plant combined with the designed controller.

in regulation system provided that it is possible to measure the size of the disturbance. Since the size of the aerodynamic drag is known, and it is constant, this theory can be applied to the satellite, even though the satellite in reality can not measure the aerodynamic drag.

To design and estimate the need of a feed-forward application, it is first important to how much the disturbances affect the system. Figure 5.8 shows a step response of the regulation system with and without the disturbances.

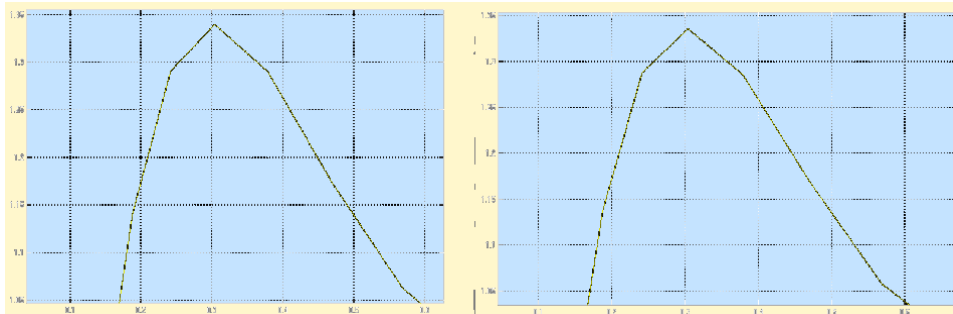


Figure 5.8: The figures shows a closeup of the step response. The graph to the left is without the effect of disturbances and the one to the right is with.

It is clearly seen that the disturbances do not affect the regulation system a lot. Besides a minor increase in the overshoot and speed of the system the disturbances do not cause a lot of damage. This is probably due to the fact that the control torque is a factor 10 larger in size than the disturbance torque. The need of a feed-forward application would not be necessary.

5.6 Design of the Controller in Z-Domain

The focus of this section will be to calculate the discrete version of the controller now that it has been designed and verified in the Laplace domain. The final controller can be expressed in the Laplace domain as seen in equation 5.21.

$$A_c(s) = \frac{Y(s)}{R(s)} = K \cdot \frac{s+a}{s+b} \Leftrightarrow Y(s) \cdot (s+b) = R(s) \cdot K \cdot (s+a) \quad (5.21)$$

By inverse Laplace the controller in equation 5.21 one get equation 5.22.

$$\dot{u} + b \cdot u = K \cdot (\dot{e} + a \cdot e) \quad (5.22)$$

By sampling the signal and applying *Eulers Method* equation 5.22 can be rewritten into equation 5.23 given the controller in discrete time.

$$\frac{u[k+1] - u[k]}{T} + b \cdot u[k] = K \cdot \left(\frac{e[k+1] - e[k]}{T} + a \cdot e[k] \right) \quad (5.23)$$

With a few calculations the equation 5.23 can be rewritten into a more practical form as seen in equation 5.24.

$$u[k+1] = u[k] - b \cdot T \cdot u[k] + K \cdot e[k+1] + K \cdot e[k] + K \cdot a \cdot e[k] \quad (5.24)$$

Where $u[k]$ and $e[k]$ simply represent the output and input of the controller to a given sample. By substituting each variable with its proper value the three controllers for the X-, Y- and Z-axis can be determined in their discrete form.

5.7 Summary

In this chapter the combined system was described in order to design the controllers. With this the effect of the cross contributions was found and they were removed as seen fit. With this simplified description of the system the controllers were first designed in the Laplace domain, using the requirements set up earlier, and then applying the root locus method to place the last pole. After the controller was described in the Laplace domain it was transformed into the Z-domain, to get the discrete controller which can be implemented. These controllers for the different axis will be tested in the next chapter.

Chapter 6

Integration and Accept test

The chapter examines how the controller, from the previous chapter, can be implemented in different environments in order to be fully verify its functionality. The controller will undergo two test, one in a highly advanced MATLAB simulation environment, provided by the AAU space team, and a practical test (accept test) on a satellite model. Furthermore, the chapter evaluates the results from the different test in order to estimate the functionality of the final controller. To summarize, the chapter will be divided into two parts examined in the following order:

- Accept Test - Practical LAB test with satellite model
- MATLAB simulation test - Integration and Results

6.1 Accept Test

The practical test of the satellite is carried out as stated in chapter 3, the test setup can also be seen there. A model of the satellite is placed within two Helmholtz coils generating a external magnetic field, 20 times stronger than the Earth's. This in effect cancels out the Earth's magnetic field, and the only thing that really affects the Satellite models actuation is the generated magnetic field.

The model of the satellite has only one magnetorquer, which means that the satellite can actuate in two axis. Furthermore the satellite is hung, in a magnet, and due to gravity the satellite is not able to rotate in this direction. In terms of the SBRF, the magnetorquer allows for actuation around the z-axis and the x-axis. The gravity on Earth keeps the rotation about the x-axis constant by proving a much larger force pulling it down than the magnetorquer can. This means that the system does not have any cross contributions, and only turns around the z-axis as the test is run. This

means that the controller is being tested under the same conditions and assumptions it was designed.

To summarize, the laboratory test is designed and carried out under the same conditions the controller was designed with; Constant external magnetic field orthogonally on the satellite, no cross contributions, due to one magnetorquer and almost no disturbance torques (no wind, solar radiation etc).

A few errors is expected in the test. The main one being that the magnetic field is much stronger than what the controller is designed for it might actuate a lot more than expected. This is due to the difference in magnetic field strength in space and on earth. Another source for errors is introduced in the suspension of the satellite model, which is a magnetic ball link. This introduces a friction into the dynamics of the satellite, with a pole located outside zero. This might cause some problems because it has not been factored into the controller design. The magnet might also cause other problems as it is placed in a powerful magnetic field and thus forces will be created when the different magnetic fields interact. The notion of having a perpendicular magnetic field is also slightly incorrect as this is only true in the starting position. Thou it is expected that the turning of 10 degrees will not cause any major disturbances, from the perpendicular position. There are also problems with the sampling frequency as the controller is designed to work at a sampling frequency of 152 Hz, but only 40 Hz is available from the video feed. This will create a delay in the controller, and might ultimately lead to instability over time.

Within the model of the satellite is an Arduino micro controller sending PWM signals into the magnet torquers of the satellite. In order to avoid cables, that might cause friction and errors in the system and so on, a wireless communication between a computer and the Arduino has been established. This means that the controller will run in MATLAB on the computer and send the control signals to the Arduino which then controls the satellite. The whole setup is placed in a camera control room, where a number of cameras measure the orientation of the satellite and send result back to the computer, which plots the results in MATLAB.

Credits for the code and hardware made for this test will go to EIT group 14GR624 at Aalborg University, who also worked on an ADCS, but specific to this model and not space.

Figure 6.1 shows the results of the test with a 10° step, so the satellite is set to rotate 10° and then hold its orientation.

It is seen from figure 6.1 that the controller manages to control the satellite quite successful. The system has a settling time which is much less then the required 30s, but it is seen that it is a bit larger then the one in the simulation in chapter 5. The controller also succeeds in keeping the satellite within a 10° precision limit and 8% of overshoot as also stated in the requirements. It is clear that a very powerful

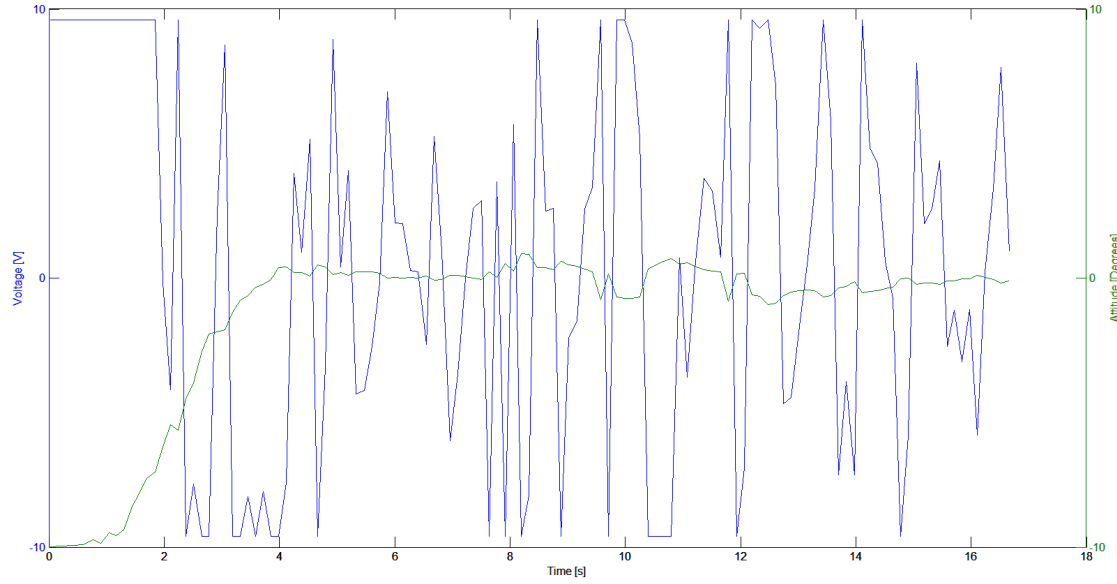


Figure 6.1: The figure shows the results of the physical satellite test, where the blue graph shows the voltage send to the magnet torquers and the green shows the orientation of the satellite.

integration takes place in the controller, which causes big spikes in the voltage as a response to small errors. This does not seem to be a problem as the satellite position is kept relatively still. It seems that, even with the deviations from the environment the controller was designed for, it works and is able to stabilise the satellite in one axis, with a constant magnetic field perpendicular to the magnetorquer.

6.2 Matlab Simulation

It has been shown that the controller works as designed, both by simulation and practical test, under the assumptions and conditions that has been set. It is now interesting to see how the controller acts in an environment more similar to space. In other words, the goal is to see and evaluate the functionality of the controller when disturbances, cross contributions etc. are included in the test.

To do this an advanced MATLAB simulation environment, that has been acquired by the AAU space team, is acquired. It was originally designed by the team behind the AAUSAT3, and credits for the simulation environment will go to them. The simulation environment is designed in such a way that it represents an actual satellite in space. Disturbances like the sun, the magnetic field and wind is contained in the simulation environment, to represent a satellite in orbit as much as possible.

The most correct way to evaluate the controller under these conditions would be to

run a number of small test, including a new disturbance or removing one assumption at a time, to see where the main problem of the controller is and how much each elements *hurts* the functionality of the controller. Unfortunately, the MATLAB environment is very complicated, and due to time limits it has not been possible to learn and edit the simulation environment in order to make a number of small simulations. Therefore, one single *crash test* simulation has been run.

This section is divided into two subsection, examined in the giving order, where each subsection focuses on:

- Implementation of the controller and test setup.
- Simulation results.

Implementation to MATLAB

The MATLAB simulation environment works by specifying the different Keplerian elements to the environment in order to create the orbit that the satellite is preforming. The next step is to specify where on the orbit lane the satellite is located (the position of the satellite in relation to the Earth, not its orientation), and how fast it is moving. The simulation environment is designed to handle a worst case scenario, so the satellite has to preform a 180° degrees rotation. The environment continues to measure and simulate the behaviour of the satellite for 4 orbits unless it is stopped manually.

In order to implement the controller in the MATLAB environment the controller needs to be represent as a function of Z in the Z-domain. Recall from the last section in chapter 5 that the controller was transformed from the S-domain to the Z-domain and written in the form a difference function as showed in equation 6.2.

$$\begin{aligned} u[k+1] - u[k] + b \cdot T \cdot u[k] &= K \cdot e[k+1] - K \cdot e[k] + K \cdot a \cdot e[k] \\ \Leftrightarrow \\ u[k] - u[k-1] + b \cdot T \cdot u[k-1] &= K \cdot e[k] - K \cdot e[k-1] + K \cdot a \cdot e[k-1] \end{aligned} \quad (6.1)$$

Equation 6.2 can easily be rewritten into a function of Z by using the close relations between difference functions and Z-functions, thereby giving equation 6.2.

$$U(z) - U(z) \cdot z^{-1} + b \cdot T \cdot U(z) \cdot z^{-1} = K \cdot E(z) - K \cdot E(z) \cdot z^{-1} + K \cdot a \cdot E(z) \cdot z^{-1} \quad (6.2)$$

With a few calculations equation 6.2 can be rewritten into the standard transfer function form, given by equation 6.3, and be directly implemented in the MATLAB satellite environment.

$$\frac{U(z)}{E(z)} = \frac{K \cdot z - (1 - K \cdot a \cdot T)}{z - (1 - b \cdot \text{cdotT})} \quad (6.3)$$

All the variables in equation 6.3 has already been determined except T , the sampling period. In order to determine this parameter, the bandwidth of the system has been analysed to a value of; $\text{BW} = 7.68$. A common design rule in regulation systems is that the sampling frequency, $f_s \geq 20 \cdot \text{BW}$, thereby providing a sampling frequency of approximately 152 Hz, which corresponds to $T = 0.0066$. Furthermore, by substituting $a = 4.87$, $b = 30$ and $K = \{K_x, K_y, K_z\}$ gives the three equations shown in equation 6.4.

$$\begin{aligned} A_{cx}(z) &= \frac{2120 \cdot z - 2058}{z - 0.8204} \\ A_{cy}(z) &= \frac{3.72 \cdot 10^5 \cdot z - 3.61 \cdot 10^5}{z - 0.8204} \\ A_{cz}(z) &= \frac{1.84 \cdot 10^8 \cdot z - 1.77 \cdot 10^8}{z - 0.8204} \end{aligned} \quad (6.4)$$

The actual implementation of the controllers in the MATLAB environment is shown on figure 6.2. Firstly the quaternion from the ADS describing the satellites actual orientation is multiplied with a quaternion describing the reference orientation, in order to estimate the error in the orientation, in the form of a quaternion. This quaternion is then re-calculated, by the theory in appendix A, into the different angels that the satellite needs to rotate in the X-, Y- and Z-axis.

Secondly, each angel is given as input to its appropriate controller, and finally the three outputs are combined into a vector which is passed on to the magnet torquers. Recall from chapter 5 the matrix describing how the three control signals affect the plant shown in equation 6.5.

$$\begin{bmatrix} 0.00150 \cdot \omega_x \cdot s \\ 0.0941 \cdot \omega_y \cdot s \\ 0.0942 \cdot \omega_z \cdot s \end{bmatrix} = \begin{bmatrix} 6.18 \cdot 10^{-5} I_y \\ 2.18 \cdot 10^{-5} I_z \\ 4.30 \cdot 10^{-7} I_x \end{bmatrix} \quad (6.5)$$

According to this matrix the control signal of the Y-controller makes the X-component of vector that is passed on to the magnet torquers, just as the X-controller makes

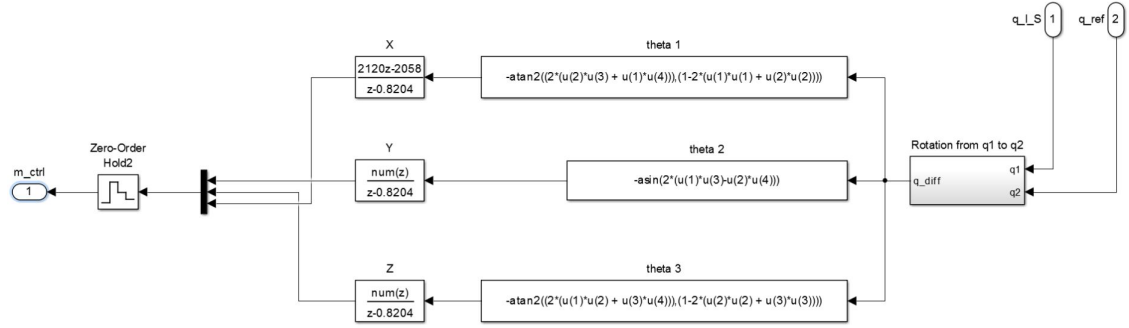


Figure 6.2: Overview of the implementation of the MATLAB satellite environment.

the Z-component and the Z-controller makes the Y-component. This information is use full when connecting the controller to the rest of the system as showed in figure 6.2.

Simulation Results

As mentioned and explained may times, the transfer function of the satellite contains a number of cross contributions that have not been taken into account in design process. This means that the controllers will never be able to fully control the satellite because when controller tries to align one axis, it changes the orientation of another axis and on, it is a bad circle that never ends. This fault can be seen in all the simulation results, especially on the angular velocity graphs where the controller keeps increasing the velocity of the satellite, in order to align the axis because they change for each regulation attempt. Figure 6.4 and 6.3 shows the angular orientation (position) and the angular velocity of the satellite in the X-axis.

It is seen on figure 6.4 that the controller affects the satellite on the X-axis changing its orientation, but in an incorrect way and never really manges to stabilize its

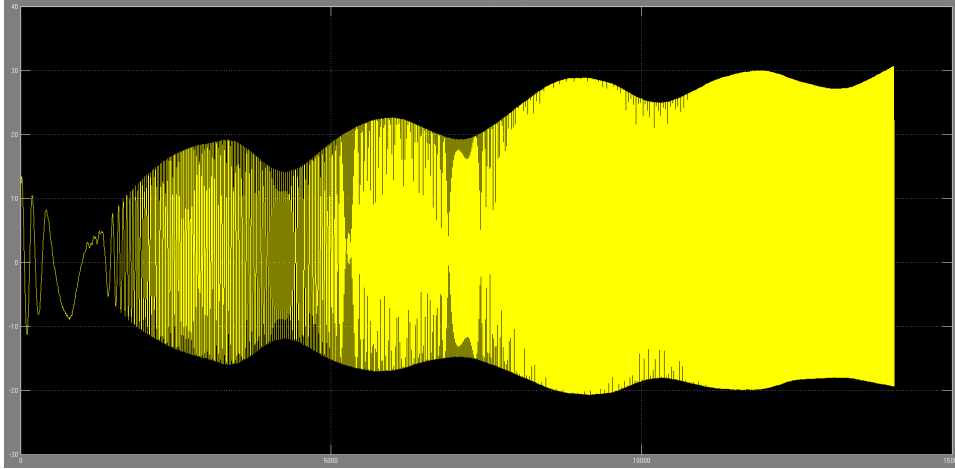


Figure 6.3: Graph displaying the angular velocity of the satellite in the X-axis during the simulation. The units of the graph on the 1.axis is seconds and 2.axis degrees/s.

orientation, which is why the angular velocity on the X-axis keeps increasing. Figure 6.6 and 6.5 shows the angular orientation (position) and the angular velocity of the satellite in the Y-axis.

Figure 6.6 shows that the controller is more successful in controlling the position of the satellite in the Y-axis, keeping it pretty stable at $\pm 80^\circ$. Unfortunately it is far from the demand of the 12° as stated in the requirement chapter. The angular velocity of the Y-axis is much similar to that of the X-axis. Figure 6.8 and 6.7 shows the angular orientation(position) and the angular velocity of the satellite in the Z-axis.

Figure 6.8 shows that the controller is also quite successful in controlling the position of the satellite in the Z-axis, keeping it stable at certain periods between $50^\circ - 120^\circ$. Unfortunately, this is also far from the demand of the 12° as stated in the requirement chapter.

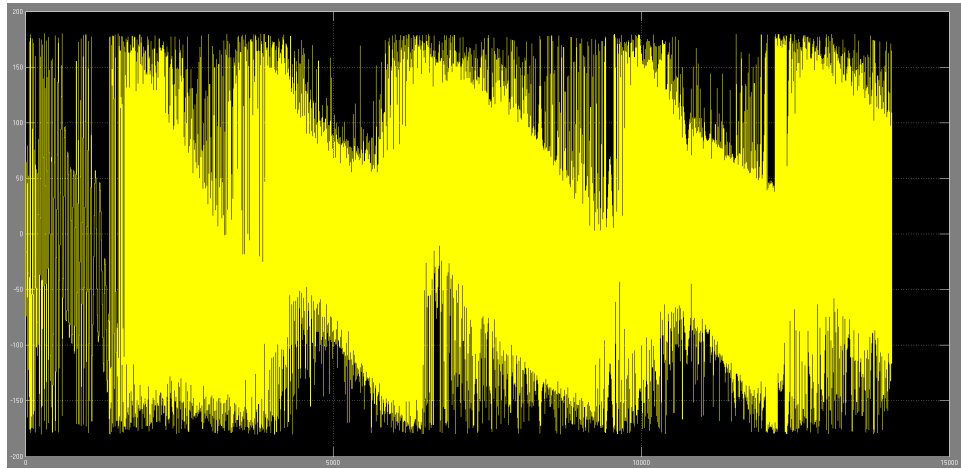


Figure 6.4: Graph displaying the angular orientation of the satellite in the X-axis during the simulation. The units of the graph on the 1.axis is seconds and 2.axis degrees.

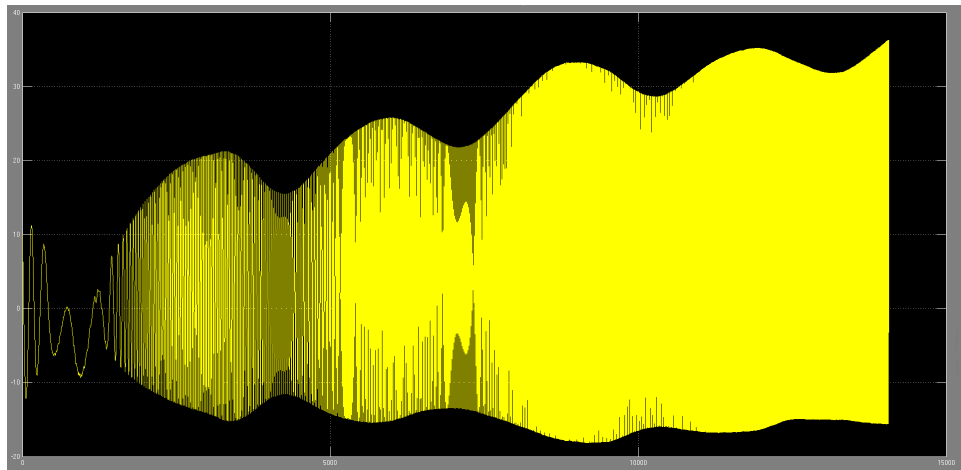


Figure 6.5: Graph displaying the angular velocity of the satellite in the Y-axis during the simulation. The units of the graph on the 1.axis is seconds and 2.axis degrees/s.

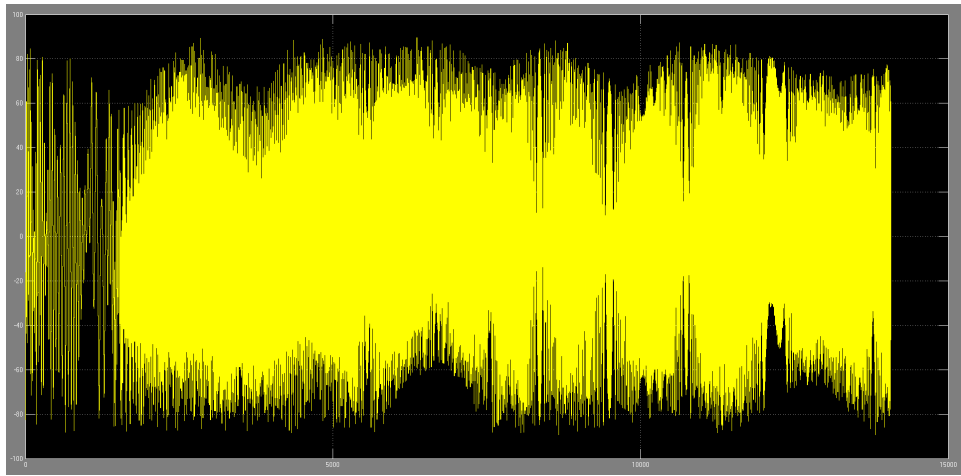


Figure 6.6: Graph displaying the angular orientation of the satellite in the Y-axis during the simulation. The units of the graph on the 1.axis is seconds and 2.axis degrees.

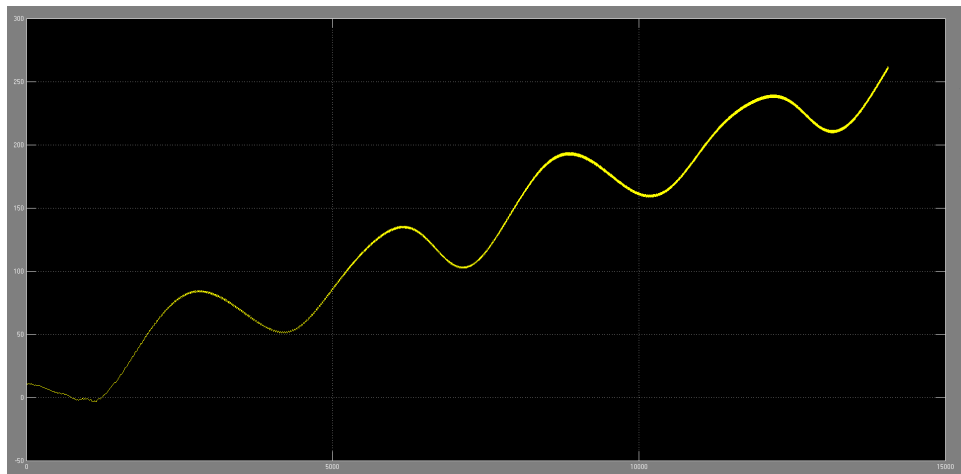


Figure 6.7: Graph displaying the angular velocity of the satellite in the Z-axis during the simulation. The units of the graph on the 1.axis is seconds and 2.axis degrees/s.

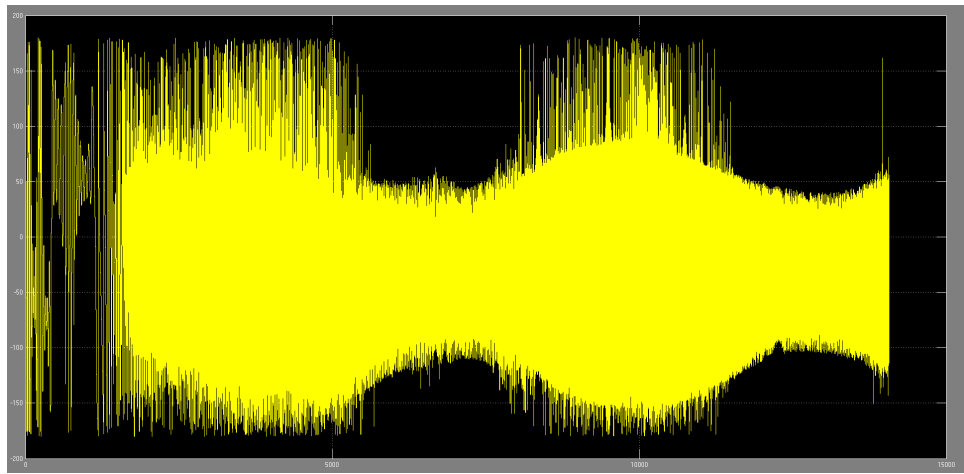


Figure 6.8: Graph displaying the angular orientation of the satellite in the Z-axis during the simulation. The units of the graph on the 1.axis is seconds and 2.axis degrees.

Chapter 7

Closure

This chapter hold the conclusion on the project and the reasons why these results were obtained, and what these means. Further the last section hold the further development to make the control of the satellite more effective.

7.1 Conclusion

It can be seen from the acceptance test in lab that the controller is successful in controlling the satellite in one axis with a constant magnetic field. This is also what the controller was designed for. The controller is even successful with the added pole that comes from the resistance in the magnetic coupling that holds the satellite, which has not been compensated in the design procedure. As it is seen in the end of the acceptance test conclusion the controller is able to fulfil the requirements set up for it in 3. The acceptance test environment is close to be implementing the assumptions taken in the design procedure with, no cross contributions due to gravity holding the axis' apart, constant magnetic field generated by the Helmholtz coils. The huge spikes of the voltage in the test when error occurs could be explained by the magnetic field generated by the coils is much greater than the Earth's which the controller is designed for, and therefore the voltage delivered to the magnetorquer is much greater than needed, and it gives a bigger control torque than anticipated. This might also be the reason that the pole created from the friction in the coupling does not introduce any larger disturbances or instabilities to the system.

As the test was moved on to test in the space environment the results were not as promising. Wild fluctuations in actuation on all axis and huge unstable responses from the system were created. There are several reasons why this is going wrong and it is not possible to say which causes it from the simulation carried out. As mentioned it would be necessary to gradually include more and more of the real

space environment to see if the satellite is controllable. What is suspected to be the major cause of the failure in the space environment is that actuation around one axis causes actuation in one other axis. Also the cross contribution from the inertia matrix not being only diagonal so the spin of the satellite will try to stabilize around another axis than the ones set up in SBRF. This in effect means, as one axis is corrected at the time, each correction of an axis removes the position of another axis. This in turn means that the applied control in the next axis is created with a wrong starting position and thus does not yield the wanted results. The third assumption used is the constant magnetic field of the earth which of course varies greatly both in intensity and orientation as described in the preliminary analysis. This will mean that the magnetic field strength anticipated is smaller or greater and voltage applied to the magnetorquers will not correspond with it and yield a wrong control torque. These three assumptions which was made during the design of the controller are seen as the main sources for the failure in controlling the satellite in space, and to further the design of a functional ADCS these must be included and considered more carefully than in this project. It can thus be concluded that it is not possible to control the satellite with the current hardware and a separate classical controller for each axis during a mission consisting of taking pictures of Earth. The cross contributions are just too great in the satellite, which means they have to be compensated in some way. As described in the start of the controller design chapter, where the transfer function of the satellite is calculated and the cross contributions can be seen, it is as mentioned a problem in the y- and z- axis that the cross contributions of the velocity in other directions is almost as great as the acceleration created in the wanted axis.

The further dwellings of the project group on how to improve the performance in controlling such a system can be seen in the next section.

7.2 Further Development

To make the project work better with the tools available to us, when discarding the cross contributions, the removed cross contributions could be subtracted in other places, such that they are still described in the dynamic equations for the satellite, but isolated to one axis. It is yet unknown how much this would help, and a quick look at the matrix in 5.6 it seems that one axis will keep having problems.

The requirements could also be eased as it is not so important how all axis of the satellite are orientated. If the camera is in the plane spanned by the x- and y-axis in SBRF, it would be sufficient to hold the spin around these axis low, and thus the cameras orientation towards Earth constant. While this is done it would not be of any great concern how fast the spin is around the z-axis, as long as it is possible to get a clear picture. With this only stabilizing two axis it might be possible to use two magnetometers to control the x- and y- axis and then use the

third magnetorquer to counteract the cross contributions between these two axis, leading to great uncertainty in the unimportant z-axis.

These two methods would probably be the best ways to improve if the same design procedure is used. Other methods would be to used other different control techniques such as state regulation. As this is still unknown to the group these other forms of control will not be described.

Bibliography

- Geomag. 2013. *Generation of the Earth's magnetic field*. http://geomag.nrcan.gc.ca/mag_fld/fld-eng.php.
- group 13gr632, AAU. 2013. *Attitude Determination and Ponting Control System for AAUSAT4*. AAU.
- Hyperphysics. 2014. *Magnetic Field of the Earth*. <http://hyperphysics.phy-astr.gsu.edu/hbase/magnetic/magearth.html>.
- IUGG. 2000. XXXX. <http://www.bgs.ac.uk/iaga/docs/DivisionV2013BusinessMeetingMinutes.pdf>.
- Larsen, Jesper A. 2014. *ADCS Lecture*.
- Noton, Maxwell. 1998. *Spacecraft Navigation and Guidance*. Springer.
- Oltrogge, Daniel L. 2011. *An Evaluation Of CubeSat Orbiatl Decay*.
- Peter Fortescue, John Stark, & Swinerd, Graham. 2003. *Spacecraft Systems Engineering*. Wiley.
- Sidi, Marcel J. 1997. *Spacecraft Dynamics and Control*. Cambridge University Press.
- Survey, British Geological. 2009. *The International Geomagnetic Reference Field*. http://nora.nerc.ac.uk/13360/1/IAGASpringer_IGRF_R5.pdf.
- Wertz, James R. 1999. *Space mission analysis and design*. Space technology library.
- Whabba, G. *A least square Estimate of Spacecraft Attitude, year = 1965*. xxx.
- Wikipedia. 2013. *Sputnik 1*. http://da.wikipedia.org/wiki/Sputnik_1.
- Wikipedia. 2014. *Quaternion*. <http://en.wikipedia.org/wiki/Quaternion>.
- Wisegeek. 2014. *The magnetic field of the Earth*. <http://www.wisegeek.com/how-strong-is-the-earths-magnetic-field.htm>.

Appendix A

Matrix Rotation Theory

This chapter examines the basic theory of rotating a vector, or set of vectors, from one coordinate system (reference frame) into another. In the following part, three different methods of rotation will be examined, which in the end will lead to a conclusion regarding which method will be used in this project. The following methods will be explained:

- Direction Cosine Matrix
- Euler Angles
- Quaternions

The different methods are examined in the above stated order.

A.1 Direction Cosine Matrix

The *Direction Cosine Matrix* is the basic method when rotating reference frames and vectors. It might not be the smartest one of the three methods, we will look into this later, but it provides a very good geometrical understanding of the rotation and can therefore be very useful to illustrate what actually happens. Furthermore, since this method is *the basic one*, it provides the necessary theoretical fundamentals to the other available methods.

Consider the coordinate system U and V as shown in figure A.1. Now imagine that one wish to rotate a vector \mathbf{v} in the system V to its corresponding vector \mathbf{u} in the U coordinate system. The direction cosine matrix (\mathbf{C}) for this rotation is defined as stated in equation A.1, which expresses a direction cosine matrix in its general form.

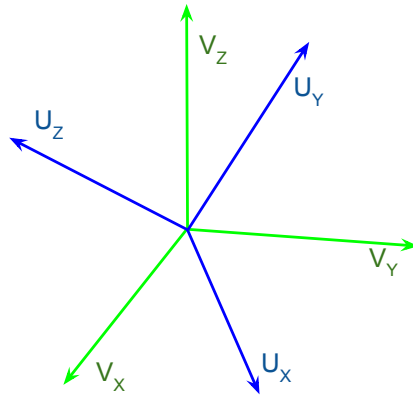


Figure A.1: The figure shows two arbitrary coordinate systems named U and V which are rotated relative to each other.

$$\begin{bmatrix} u_1 \\ u_2 \\ u_3 \end{bmatrix} = \begin{bmatrix} C_{11} & C_{12} & C_{13} \\ C_{21} & C_{22} & C_{23} \\ C_{31} & C_{32} & C_{33} \end{bmatrix} \cdot \begin{bmatrix} v_1 \\ v_2 \\ v_3 \end{bmatrix} \quad (\text{A.1})$$

Each element in the matrix \mathbf{C} can be calculated as the cosine of the angle between the two unit vectors of the vectors \mathbf{v} and \mathbf{u} as equation A.2 illustrates.

$$C_{ij} = \mathbf{u}_i \bullet \mathbf{v}_j \quad (\text{A.2})$$

As a result of the way a direction cosine matrix is defined, it is seen that a direction cosine matrix is *orthonormal*. This gives the matrix the following property $\mathbf{A}^{-1} = \mathbf{A}^T$, which is very useful. Consider the example that we want to rotate a vector from the U reference frame to the V reference frame, because of the orthonormal property it follows that: $\mathbf{V}\mathbf{R} = \mathbf{U}\mathbf{R}^{-1} = \mathbf{U}\mathbf{R}^T$.

A.2 Euler Angles

The next method, or step when talking about rotation, is to introduce *The Euler Angels*, which are closely linked to the direction cosine matrix. Consider the special case of the direction cosine matrix where we want to keep one of the vector components fixed and only turn the components of the other axis. Let α , β and γ express

the angular rotation around the X-, Y- and Z-axis. The rotation around each axis can be expressed with equation A.3.

$$\begin{aligned}\mathbf{R}_x &= \begin{bmatrix} 1 & 0 & 0 \\ 0 & \cos(\alpha) & \sin(\alpha) \\ 0 & -\sin(\alpha) & \cos(\alpha) \end{bmatrix} \\ \mathbf{R}_y &= \begin{bmatrix} \cos(\beta) & 0 & -\sin(\beta) \\ 0 & 1 & 0 \\ \sin(\beta) & 0 & \cos(\beta) \end{bmatrix} \\ \mathbf{R}_z &= \begin{bmatrix} \cos(\gamma) & \sin(\gamma) & 0 \\ -\sin(\gamma) & \cos(\gamma) & 0 \\ 0 & 0 & 1 \end{bmatrix}\end{aligned}\tag{A.3}$$

The three matrices in equation A.3 are called *The Elementary Rotations* and can be derived using the theory of the direction cosine matrices. Once again, consider that we want to rotate a vector from one reference frame into another. This can be done by combining the matrices from equation A.3 in different ways. This is due to the fact that matrix computation is non-commutative, thereby giving a different result depending on how the combination is done. They can be combined in 12 ways to be specific, e.i. the *3-2-1 rotation* shown in equation A.4.

$$\mathbf{R} = \mathbf{R}_x(\alpha) \cdot \mathbf{R}_y(\beta) \cdot \mathbf{R}_z(\gamma)\tag{A.4}$$

Eigenaxis Rotation Theorem of Euler

Besides expressing a rotation in the form of *Euler Angles*, Euler took the concept of rotation even further and developed a theorem known as *Euler's Eigenaxis Rotation* or *Euler's principal axis*. This theorem describes the rotation with the use of a vector instead of a matrix, which is more simple calculate on than a 3x3 matrix, such as a direction cosine matrix.

The exact theorem is given as followed:*A rigid body or coordinate frame fixed in a point P can be brought from any arbitrary initial orientation to an arbitrary final orientation by a single rotation θ about a principal axis $\hat{\mathbf{e}}_e$ through the point P.*[Larsen, 2014]. This axis or vector can be calculated from a direction cosine matrix with equation A.5.

$$\hat{\mathbf{e}}_e = \frac{1}{2 \cdot \sin(\theta)} \cdot \begin{bmatrix} C_{23} - C_{32} \\ C_{31} - C_{13} \\ C_{12} - C_{21} \end{bmatrix} \quad \theta \neq \pm n \cdot 180 \quad (\text{A.5})$$

The reverse calculation, from $\hat{\mathbf{e}}_e$ to a direction cosine matrix, can also be done using equation A.6

$$\mathbf{C}(\hat{\mathbf{e}}_e, \theta) = \cos(\theta) \cdot \mathbf{I} + \left(1 - \cos(\theta) \cdot \hat{\mathbf{e}}_e \cdot \hat{\mathbf{e}}_e^T - \sin(\theta) \cdot \mathbf{E} \right)$$

Where :

$$\mathbf{E} = \begin{bmatrix} o & -e_{e,3} & e_{e,2} \\ e_{e,3} & 0 & -e_{e,1} \\ -e_{e,2} & e_{e,1} & 0 \end{bmatrix} \quad (\text{A.6})$$

A.3 Quaternion

A quaternion, also known as a hyper-complex number, is a complex number which consists of a real part and three imaginary parts i, j and k . The mathematical relation between real numbers and the different imaginary parts of the quaternion is defined as stated in equation A.7[Wikipedia, 2014].

$$\begin{aligned} i^2 = j^2 = k^2 = i \cdot j \cdot k &= -1 \\ \Downarrow \\ i \cdot j &= k, \quad j \cdot i = -k \\ j \cdot k &= i, \quad k \cdot j = -i \\ k \cdot i &= j, \quad i \cdot k = -j \end{aligned} \quad (\text{A.7})$$

A quaternion can also be described as a vector. In case the vector has *the unit length*: $q_{1:3}^* \cdot q_{1:3} + q_4 = 1$, where $q_{1:3} = [q_1 : q_2 : q_3]^T$, the vector can geometrically be interpreted as a four dimensional sphere where a rotation is describing a trajectory on the surface of this sphere. Quaternions used as a rotation tool, is closely linked to Euler's Eigenaxis Theorem and it can be shown that a rotation in the form of quaternion can be described by equation A.8.

$$\mathbf{q} = \begin{bmatrix} \hat{\mathbf{e}}_e \cdot \sin\left(\frac{\theta}{2}\right) \\ \cos\left(\frac{\theta}{2}\right) \end{bmatrix} \quad (\text{A.8})$$

In order to make a whole series of rotations, one simply multiplies different direction cosine matrices together, as shown earlier. The same property applies to quaternions. Multiplication with quaternions is mathematically defined as stated in equation A.9[Larsen, 2014], it is seen that the procedure is the same as with regular complex numbers.

$$\begin{aligned} \mathbf{q} \otimes \mathbf{p} &= (\mathbf{i}q_1 + \mathbf{j}q_2 + \mathbf{k}q_3 + q_4) \cdot (\mathbf{i}p_1 + \mathbf{j}p_2 + \mathbf{k}p_3 + p_4) \\ &= \mathbf{i}^2 q_1 p_1 + \mathbf{i}\mathbf{j}q_1 p_2 + \mathbf{i}\mathbf{k}q_1 p_3 + \mathbf{i}q_1 p_4 \\ &\quad + \mathbf{j}^2 q_2 p_2 + \mathbf{j}\mathbf{i}q_2 p_1 + \mathbf{j}\mathbf{k}q_2 p_3 + \mathbf{j}q_2 p_4 \\ &\quad + \mathbf{k}^2 q_3 p_3 + \mathbf{k}\mathbf{i}q_3 p_1 + \mathbf{k}\mathbf{j}q_3 p_2 + \mathbf{k}q_3 p_4 \\ &\quad + \mathbf{i}q_4 p_1 + \mathbf{j}q_4 p_2 + \mathbf{k}q_4 p_3 + q_4 p_4 \\ &\quad \Downarrow \\ \mathbf{q} \otimes \mathbf{p} &= \mathbf{i}q_1 p_4 - \mathbf{j}q_1 p_3 + \mathbf{k}q_1 p_2 - q_1 p_1 \\ &\quad \mathbf{i}q_2 p_3 + \mathbf{j}q_2 p_4 - \mathbf{k}q_2 p_1 - q_2 p_2 \\ &\quad \mathbf{i}q_3 p_2 + \mathbf{j}q_3 p_1 - \mathbf{k}q_3 p_4 - q_3 p_3 \\ &\quad \mathbf{i}q_4 p_1 + \mathbf{j}q_4 p_2 - \mathbf{k}q_4 p_3 - q_4 p_4 \end{aligned} \quad (\text{A.9})$$

Just as the case with direction cosine matrices and Euler angels, quaternion multiplication is non-commutative which result in the fact that the order in which quaternions are multiplied together produces different rotation. Furthermore, quaternions are unitary ($\mathbf{A}^{-1} = \mathbf{A}^{T*}$) thereby giving the following ability: ${}^a\mathbf{q} = {}^b\mathbf{q} \otimes_a^b \mathbf{q} \Leftrightarrow {}^b\mathbf{q} = {}^a\mathbf{q} \otimes_a^b \mathbf{q}^{-1} = {}^a\mathbf{q} \otimes_a^b \mathbf{q}^{T*}$

Quaternions and Direction Cosine Matrices

Because of the connection between Euler's Rotation Theorem and quaternions, there exist a close link between direction cosine matrices and quaternions as well. It is therefore possible to convert from one *form* into another. This is very practical because the each method provides different advantages and disadvantages in different situations.

Normally when designing a rotation algorithm e.i a matrix which rotates vectors/matrices from one coordinate system into another, the first step is to design it in form of a

direction cosine matrix, because this offer a more intuitive perspective of the rotation, and then convert it into a quaternion. The conversion can be done by equation A.3[Larsen, 2014].

$$\mathbf{q}_{1:3} = \begin{bmatrix} q_1 \\ q_2 \\ q_3 \end{bmatrix} = \begin{bmatrix} \hat{e}_{e,1} \cdot \sin\left(\frac{\theta}{2}\right) \\ \hat{e}_{e,2} \cdot \sin\left(\frac{\theta}{2}\right) \\ \hat{e}_{e,3} \cdot \sin\left(\frac{\theta}{2}\right) \end{bmatrix} = \frac{1}{4 \cdot q_4} \cdot \begin{bmatrix} C_{23} - C_{32} \\ C_{31} - C_{13} \\ C_{12} - C_{21} \end{bmatrix} \quad 0 \leq \theta \leq 180 \quad (\text{A.10})$$

where :

$$q_4 = \frac{1}{2} \cdot (\text{Trace}(\mathbf{C}) + 1)^{\frac{1}{2}}$$

The reverse calculation from a quaternion to a direction cosine matrix can be done by equation A.3[Larsen, 2014].

$$\mathbf{C}(\mathbf{q}_{1:3}, q_4) = \left(q_4^2 - \mathbf{q}_{1:3}^{T*} \cdot \mathbf{q}_{1:3} \right) \cdot \mathbf{I} + 2 \cdot \mathbf{q}_{1:3} \cdot \mathbf{q}_{1:3}^{T*} - 2 \cdot q_4 \cdot \mathbf{Q} \quad (\text{A.11})$$

where :

$$\mathbf{Q} = \begin{bmatrix} 0 & -\hat{e}_{e,3} & \hat{e}_{e,2} \\ \hat{e}_{e,3} & 0 & -\hat{e}_{e,1} \\ -\hat{e}_{e,2} & \hat{e}_{e,1} & 0 \end{bmatrix} \cdot \sin\left(\frac{\theta}{2}\right)$$

A.4 Comparison and Conclusion of the Methods

This section summarizes the key elements from the previous sections. Direction cosine matrices offer a very intuitive and practical interpretation of a rotation, thereby making it useful in analysis. On the implementation level direction cosine matrices may not be the best option. They are heavy to store memory wise, compared to the other methods (3x3 matrix vs. vector), especially because one matrix is required to describe the rotation around each axis, where the Euler Angles and Quaternions are more *compressed*.

The Euler angles also offer a very intuitive interpretation of the rotation. Furthermore, they are easier to store and compute than the direction cosine matrix. The problem though is that singularities may occur when using the Euler angles method, especially in derivative terms from kinematic or dynamic equations. Quaternions does not suffer from this and are very computation friendly because they only contain multiplication.

Therefore the normal practice, as mentioned, is to use direction cosine or Euler angels form the analytical parts of a problem (the modelling) and then convert them into quaternions for practical use or final implementation.

Appendix B

Journal for measurement of magnetotorquers

B.1 Purpos

To verify the model used for the coils in the magnetotorquer, by placing the coil in a permanent magnetic field and passing a current through it. This allows for a measurement of the angle the coils take moves from vertical. The force exerted on the coil can then be calculated with the one being gravity and the other presumed to be the one described by Laplace's law.

B.2 Used equipment

Test object A coil from the magnetotorquer.

Other test equipment Fixture

A horse shoe permanent magnet, 300 gauss.

A power supply.

Wires for connections.

A goniometer. (for measuring angles)

B.3 Measurement arrangement

The measurement arrangement can be seen on figure B.1. The coil is placed with one part between the poles of the horseshoe magnet, by hanging it in strings so it

can move freely. The coil should be able to move back and forth as easily as possible. The power supply is connected to the coil with soft wires so that it does not inhibit the coils movement.

Before the measurement the gravitational force on the coil should be measured. In Aalborg this is 0.23 N. This measurement is done by suspending the coil in a newton meter and waiting for it to settle.

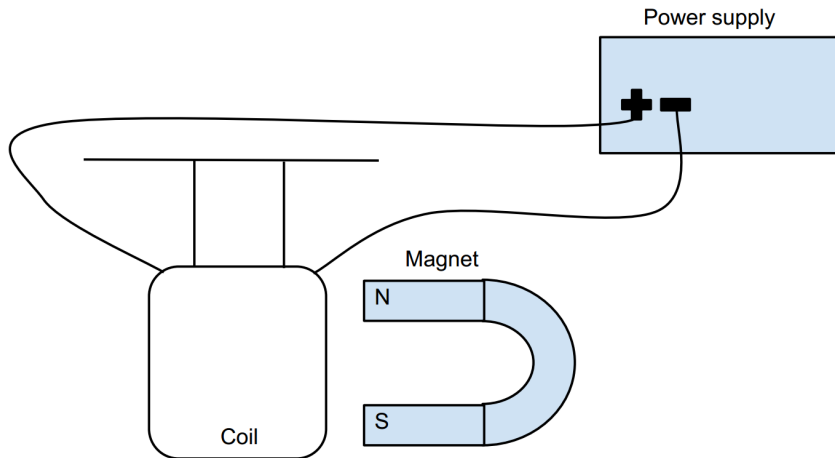


Figure B.1: The figure shows the configuration of the experiment.

B.4 Measurement procedure

The goniometer is placed and the angle is 0 degrees from vertical, otherwise the strings to the coils should be reattached to get 0 degrees.

Power is connected to the coil and the voltage is slowly increased for a larger current through the coil.

The current is noted when the angle reaches 5 degrees, and from every degree it increases from here on.

The experiment is ended when the coil has moved so much it starts to get out of the magnetic field of the magnet or it hits the magnet.

B.5 Data processing

The angle of the coil can be described via trigonometry as seen in B.1. Where F_i is the force from the current and F_g is the gravitational force measured to 0.23 N in Aalborg. The two forces can be seen on figure B.1. This method is used backwards

on the measured results to calculate the force exerted on the coil when a current is passed through it.

$$\tan\left(\frac{F_i}{F_g}\right) = \theta \quad (\text{B.1})$$

The calculated forces on the coil are inserted into the table with the results as an extra column and next to it, will be the percentile deviations from measured data to the expected.

B.6 Results

Current mA	Measured θ deg	"Measured force" deg	Calculated force N	Percentile deviation N
37	5 deg	0.0201	0.0208	-3.3 %
45	6 deg	0.0241	0.0253	-4.5 %
54	7 deg	0.0282	0.0303	-7.0 %
59	8 deg	0.0323	0.0337	-4.2 %
65	9 deg	0.0364	0.0365	-0.4 %
73	10 deg	0.0405	0.0410	-1.2 %
82	11 deg	0.0447	0.0461	-3.0 %
88	12 deg	0.0488	0.0495	-1.2 %
97	13 deg	0.0531	0.0545	-2.6 %

B.7 Error sources

The magnet used is an old magnet, which means the magnetic field in it might have weakened from its manufacturing. This could be measured but no magnetometer is available. This is a very plausible explanation for the deviations because they all seem to be equally off from the calculated angles.

Errors in measurement will also have contributed some error as the angle of the coil to vertical is measured by hand, and the goniometer might not have been aligned correctly.

The magnetic field stops being perpendicular to the current as the coil starts to tilt. The perpendicular magnetic field is assumed in this experiment and therefore a fall in accuracy is expected in the last results if the angle between the magnetic field and the current gets large enough. This is seen from the sine term in the equation, with an angle of the coil between 5 and 13 degrees the angle between current and magnetic

field is 85 and 77 degrees. The sine terms for these are 0.99 and 0.97 respectively, and therefore this minor error can be ignored.

B.8 Conclusion

From the results section it can be seen that the deviation in the results from what was expected is fairly constant. The negative deviation throughout the experiment is attributed to the bar magnet which is old, and might have lost a bit of its magnetic strength. For a more precise measurement the field strength of the magnet should be measured.

It is concluded that Laplace's law generates the expected forces in the coil. This is when the angle between the magnetic field and the current is small (5-13 degrees), so the sine term can be neglected as it is close to 1.

It can be concluded the model used for the coils is sufficiently accurate to the real world for the design of the controller. Therefore Laplace's law will be used for the model of the magnetorquers.

Appendix C

Journal of measurement for the inertia matrix

C.1 Purpose

To verify the inertia matrix obtained from the inventor program by measuring the first diagonal element of the inertia matrix for a mass dummy of the satellite. This is done by measuring the inertia on the first positions of the diagonal matrix and then comparing this with the results obtained from Inventor.

C.2 Used equipment

Test object Mass dummy of the AAUSAT3

Other test equipment Fixture

Motor

Oscilloscope

Power supply

Tachometer

C.3 Measurement arrangement

The measurement arrangement can be seen on figure C.1. The mass dummy is fixed on a motor with known inertia and time constant. The mass dummy is fixed so the center of mass is in the axis of spin. The motor is connected to a power supply. A

tachometer will be connected to measure the speed of the motor. When the motor is at a constant speed it will be shut off and the tachometer is read until the motor stops rotating. The inertia of the mass dummy can then be calculated.

In this experiment a motor with a built in tachometer is used, and the time will be kept by the oscilloscope, from which the data will be saved to a USB for further analysis.

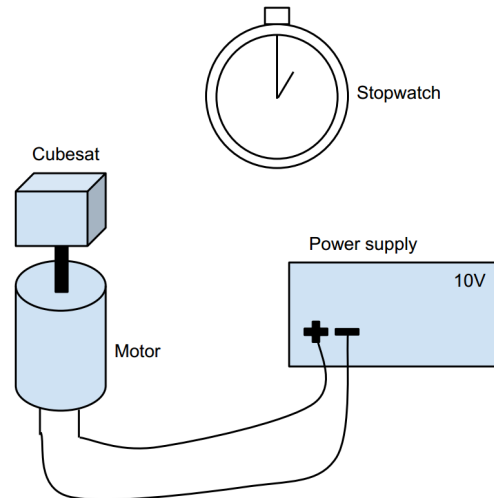


Figure C.1: The figure shows the configuration of the experiment.

C.4 Measurement procedure

The mass dummy is fixed on the motor.

The motor is connected to power.

Power is turned on for the motor.

When the motor is spinning with a constant speed, power is turned off.

While power is turned off a stopwatch is turned on.

When the cubeSAT stops moving the time on the watch is noted.

C.5 Results

First the viscous resistance of the motor is calculated. This is done as the mechanical time constant is equal to the inertia of the motor divided by the resistance.

$$\tau_{mechanical} = \frac{J_{motor}}{B_{motor}} \quad (C.1)$$

Where:

$\tau - motor$ is the motor constant $13.2s$

J_{motor} is the inertia in the motor equal to $7.4 \cdot 10^{-5} m^2 \cdot kg$

B_{motor} is the viscous resistance of the motor $5.6 \cdot 10^{-6} \frac{m^2 \cdot kg}{s}$

The exponential function created from exponential regression on the data yields the function

$$f(x) = 7.4 \cdot 10^7 e^{-7 \cdot 10^{-4}x}$$

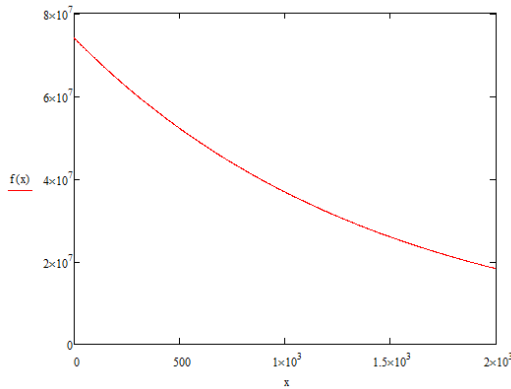


Figure C.2: The figure shows the exponential drop in rotation speed of the motor with the mass dummy added.

The time constant can be found from the function of the speed, and is the time that it takes for the speed to decrease 63 %.

The new time constant is found to be 660 seconds. When the new total inertia is calculated it gives the total inertia to be $3.7 \cdot 10^{-3} m^2 \cdot kg$. When the inertia from the motor is subtracted the added inertia is $3.6 \cdot 10^{-3} m^2 \cdot kg$.

C.6 Error sources

Placement of the center of mass of the cubeSAT right in the axis of spin on top of the motor. If the axis does not go through the center of mass the measurement will be off. Because the distance to the point mass from the axis of spin is squared when calculating the inertia, this means that the offset will grow quickly.

This might be helped by taking several measurements moving the cubeSAT slightly, and used the smallest moments of inertia found.

The motor is old, and both the bearing in the motor and the tachometer could have obtained errors over time.

C.7 Conclusion

The diagonals that can be tested are the two first positions of the inertia matrix. The value of this position is $4.8 \cdot 10^{-3} m^2 \cdot kg$ as described in section 4.2. This is approximately $\frac{1}{3}$ too little compared to the measured inertia. It is assumed that this fault is obtained as a combination of errors in the model created in inventor and the error sources in the experiment. The fact that the inertia obtained is of same magnitude and relatively close, compared to other estimates of the inertia matrix made, it is considered to be the best option to use the inertia matrix from Inventor. This is done due to the fact that it is almost impossible to find the cross contributions due to non symmetry in the satellite, and thereby find out how large these cross contributions are. Therefore the inertia matrix from Inventor will be further used in the design of the controller.

Appendix D

Controller Results and Simulations

This chapter contains all the controller results and simulations.

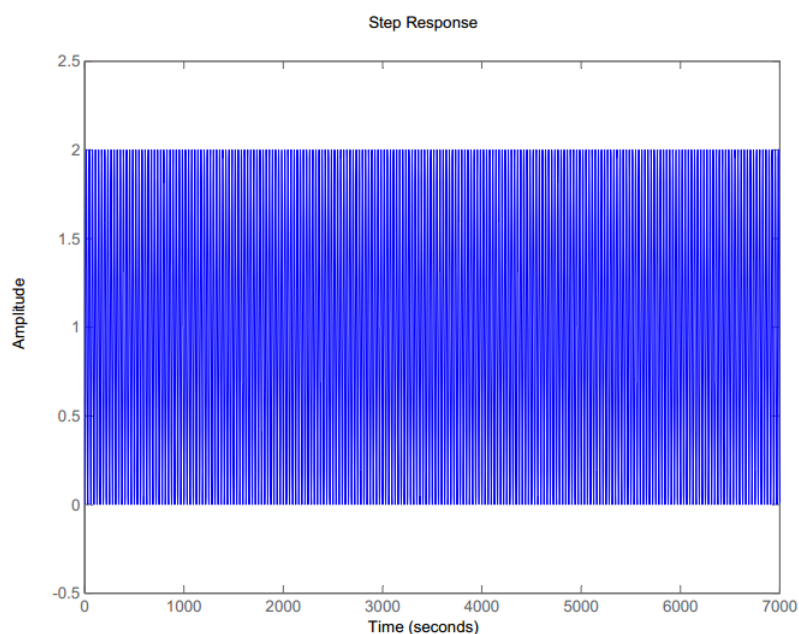


Figure D.1: The figure shows the step response of the X-axis transfer function without the controller.

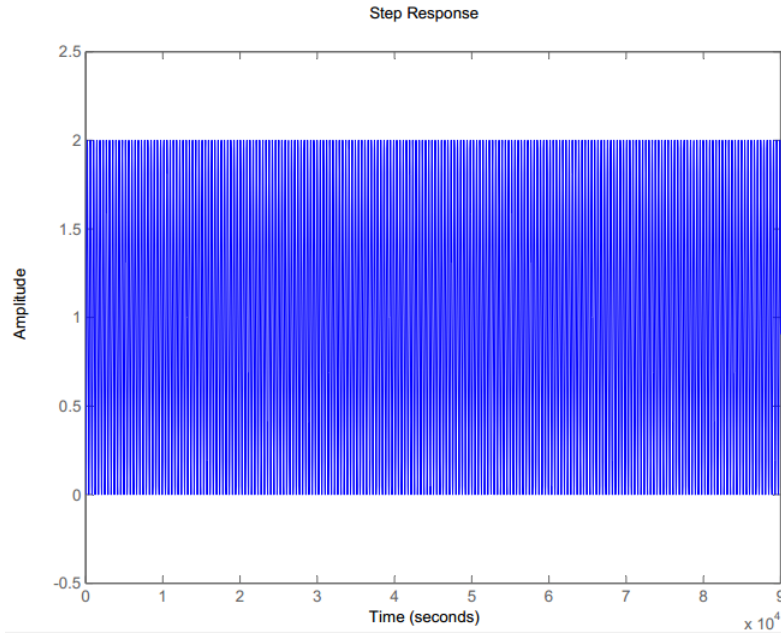


Figure D.2: The figure shows the step response of the Y-axis transfer function without the controller.

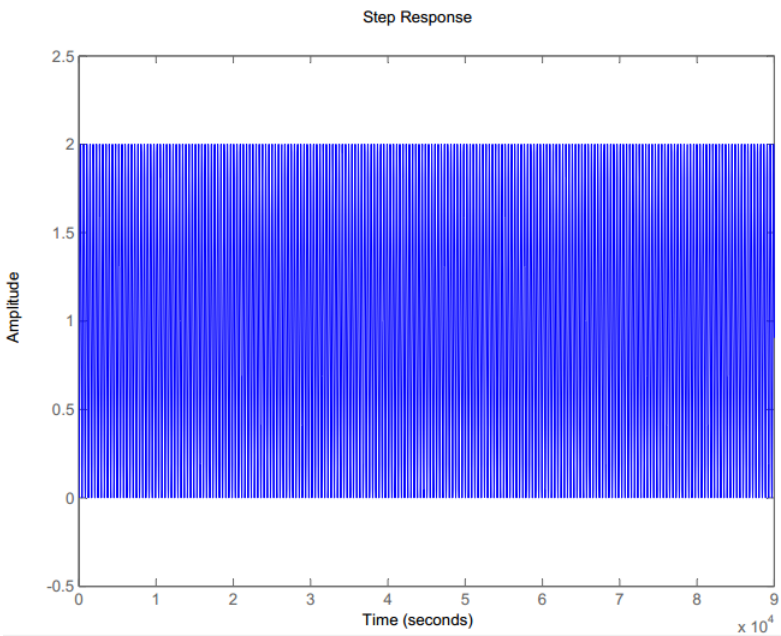


Figure D.3: The figure shows the step response of the Z-axis transfer function without the controller.

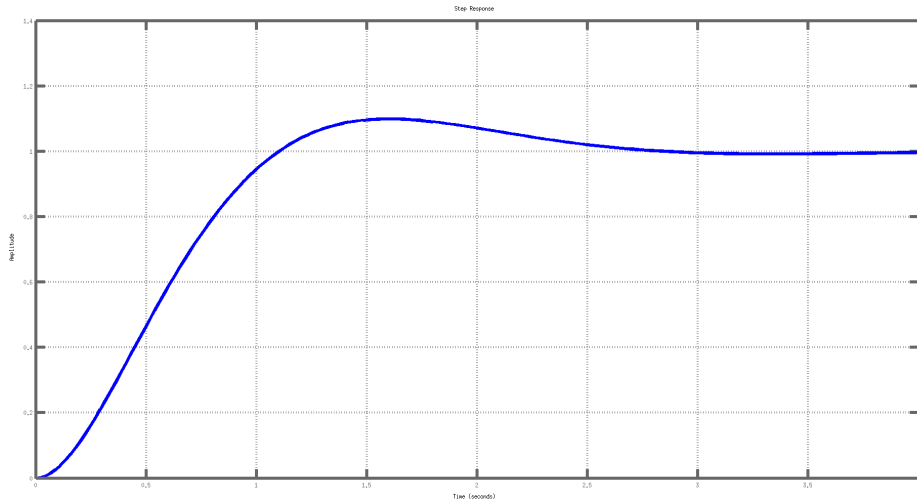


Figure D.4: The figure shows the step response of the X-axis transfer function with the controller.

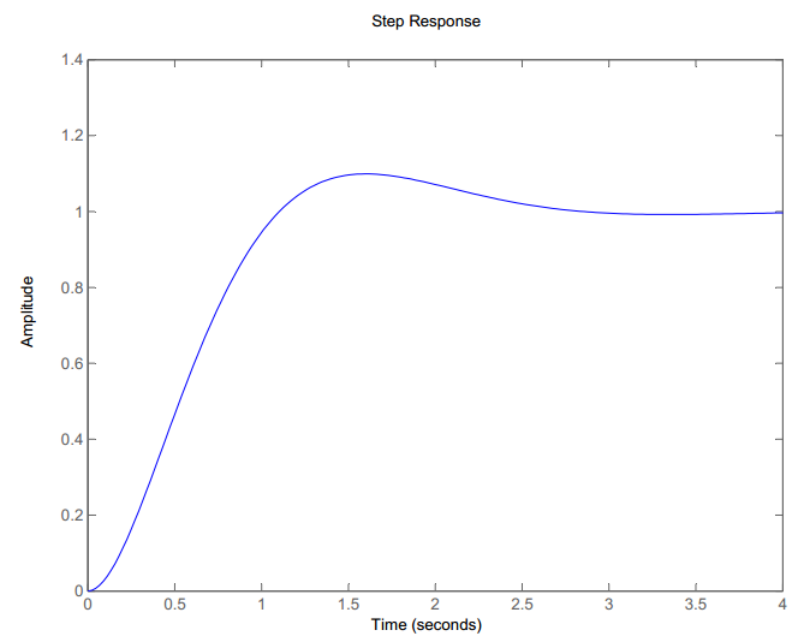


Figure D.5: The figure shows the step response of the Y-axis transfer function with the controller.

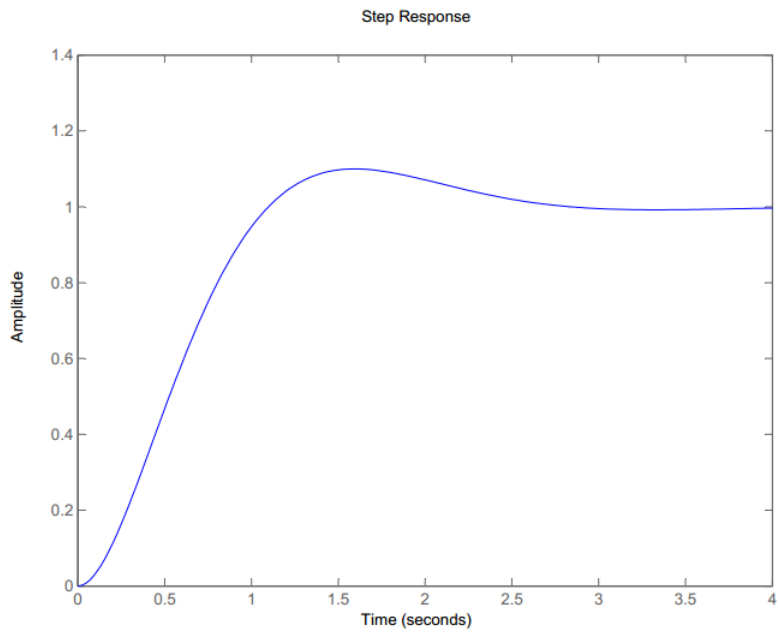


Figure D.6: The figure shows the step response of the Z-axis transfer function with the controller.

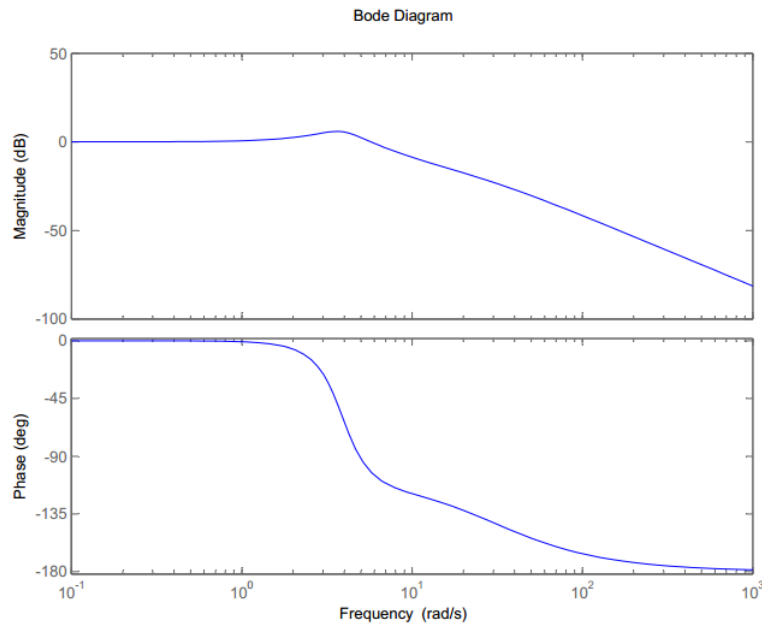


Figure D.7: The figure shows the closed loop frequency response of the X-axis system.

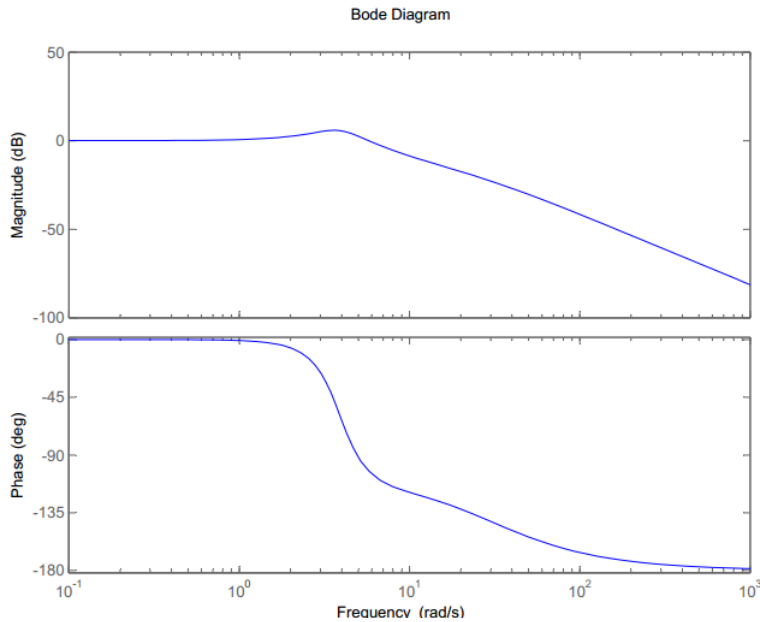


Figure D.8: The figure shows the closed loop frequency response of the Y-axis system.

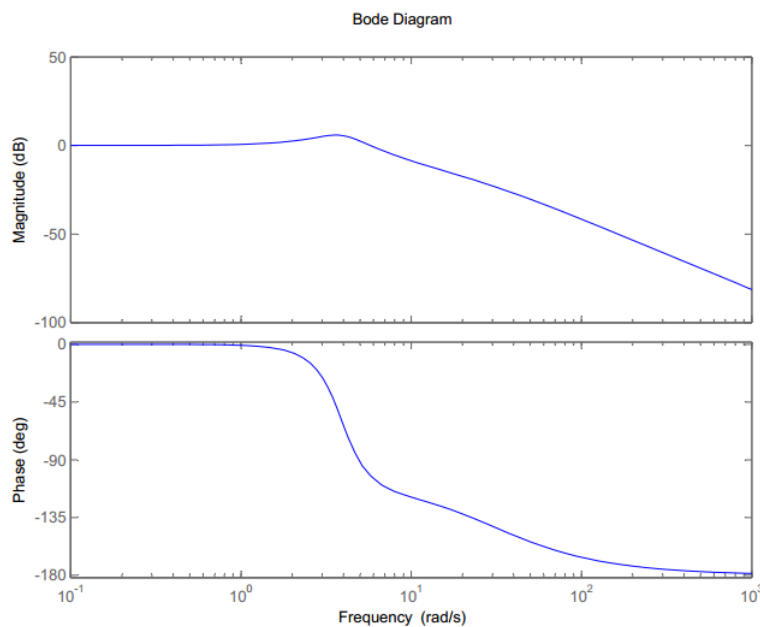


Figure D.9: The figure shows the closed loop frequency response of the X-axis system.

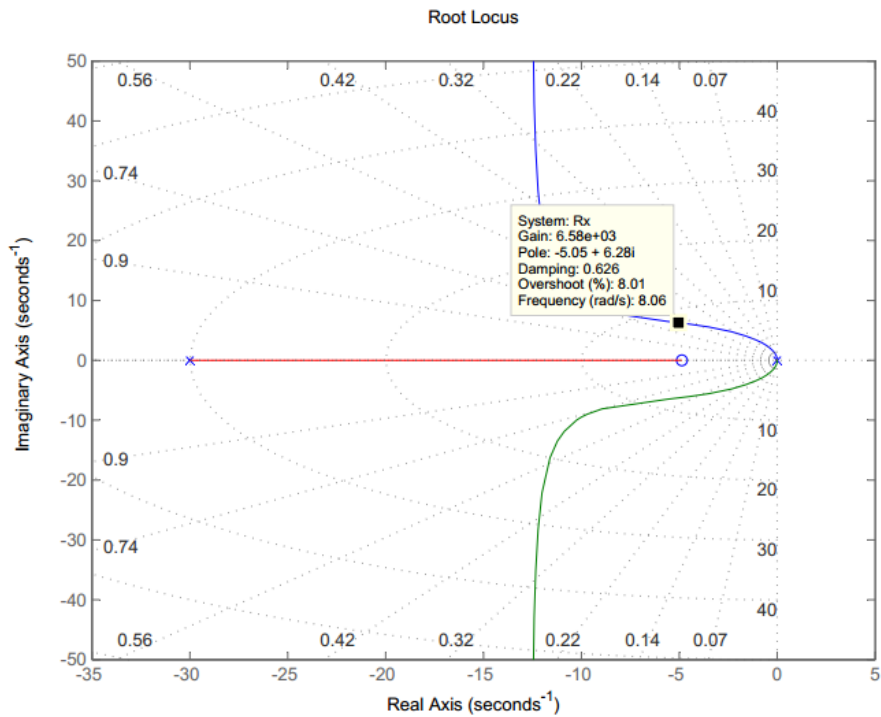


Figure D.10: The figure shows the root locus of the X-axis system..

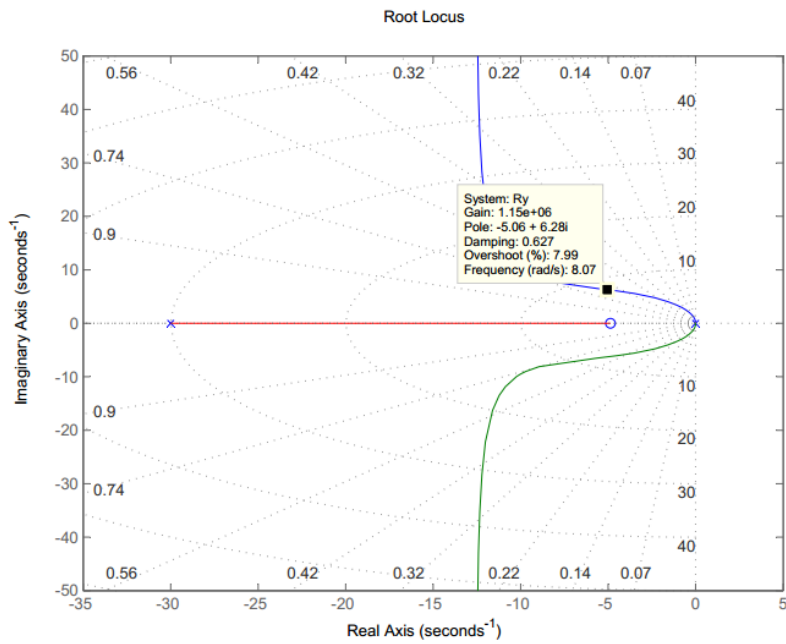


Figure D.11: The figure shows the root locus of the Z-axis system.

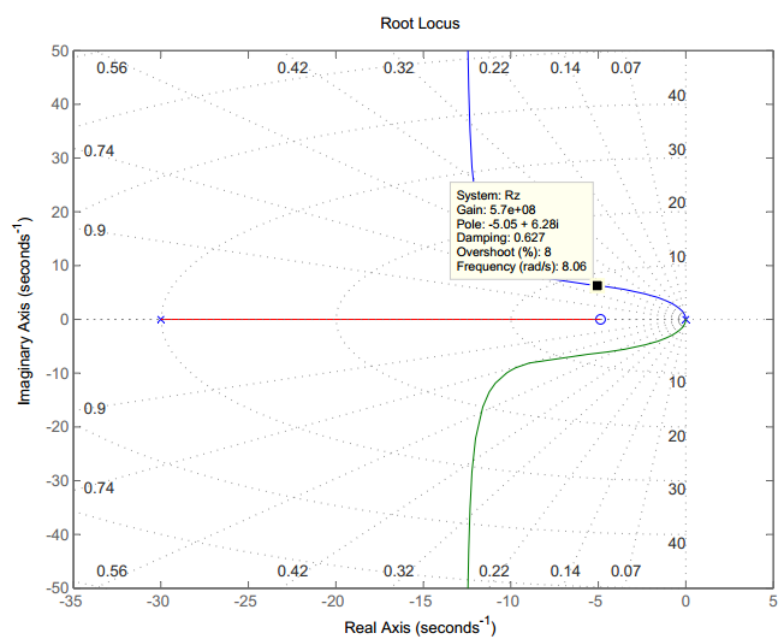


Figure D.12: The figure shows the root locus of the Z-axis system.